Exploring the Phase Diagram of V-QCD with Neutron Star Merger Simulations

Christian Ecker

Utrecht
19 January 2023

Based on 2112.12157 (PRX) and 2205.05691 (SciPost) with
Tuna Demircik, Matti Järvinen, Luciano Rezzolla, Samuel Tootle and Konrad Topolski

and

2203.14974 (ApJL), 2207.04417 (ApJL) and 2209.08101 (MNRAS) with
Sinan Altiparmak and Luciano Rezzolla

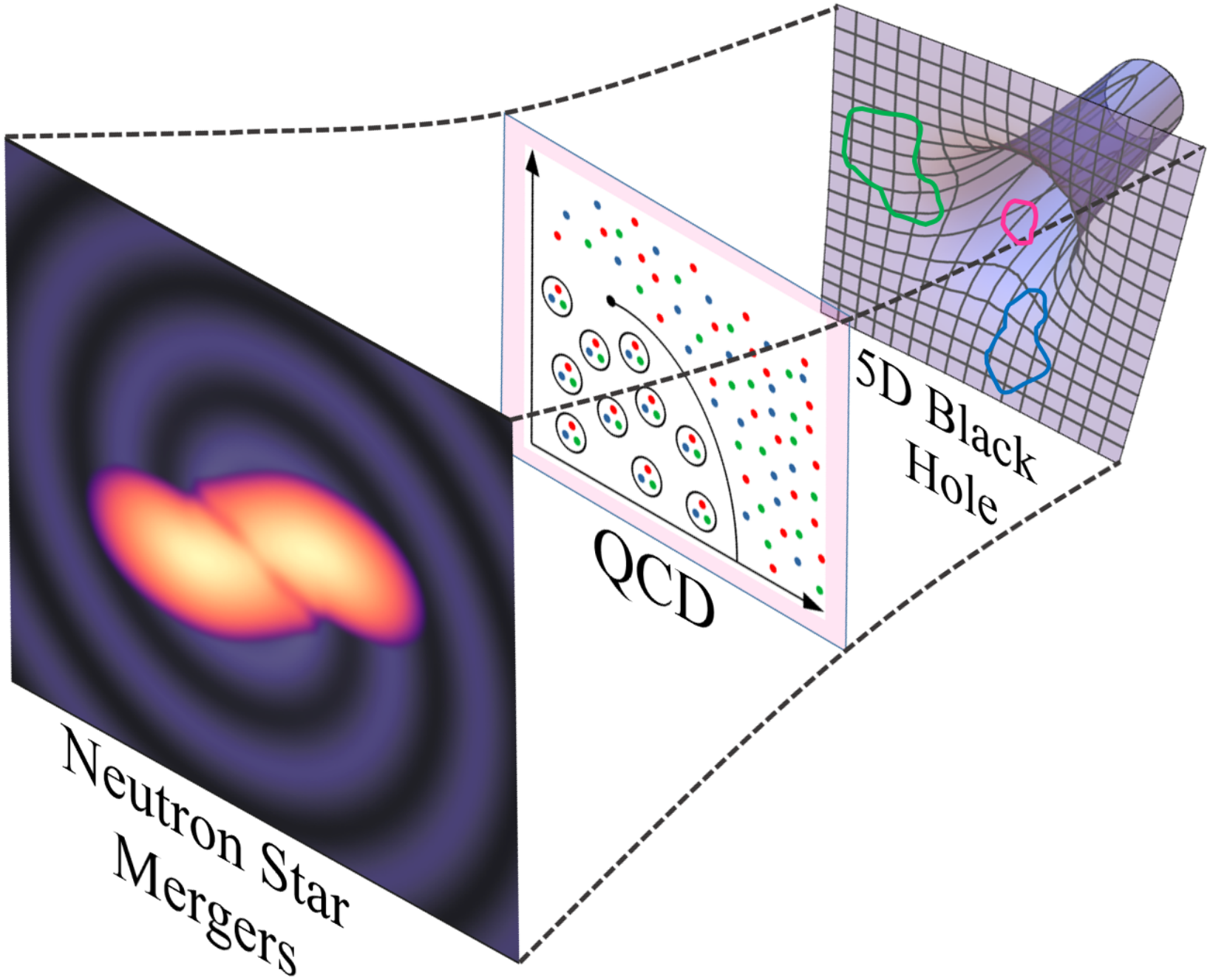
Neutron Star
Mergers
QCD
5D Black
Hole

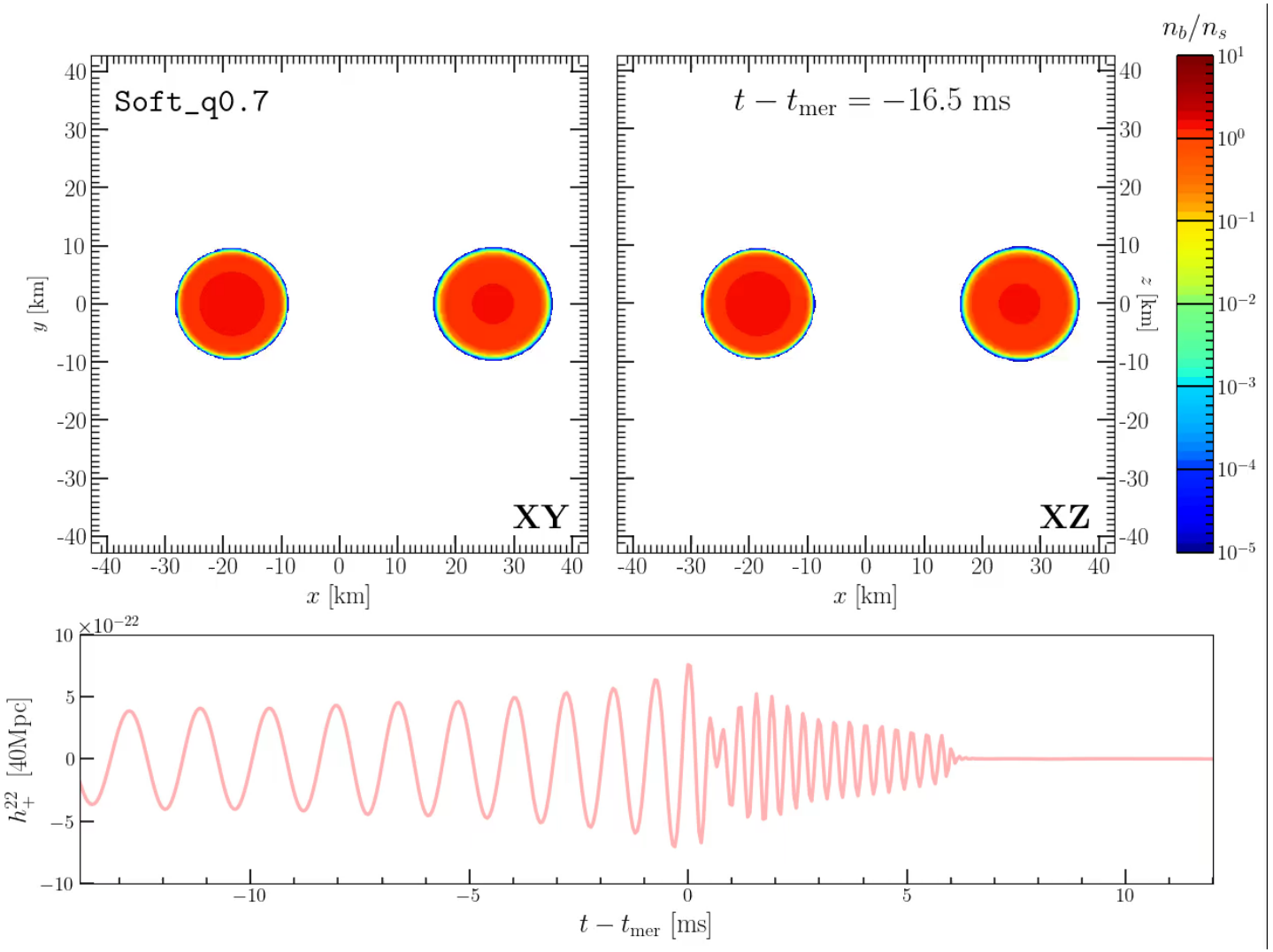
Soft_q0.7
$t - t_{\rm mer} = -16.5$ ms
XY
XZ
y [km]
x [km]
z [km]
n_b/n_s
h_+^{22} [40Mpc]
$\times 10^{-22}$
$t - t_{\rm mer}$ [ms]

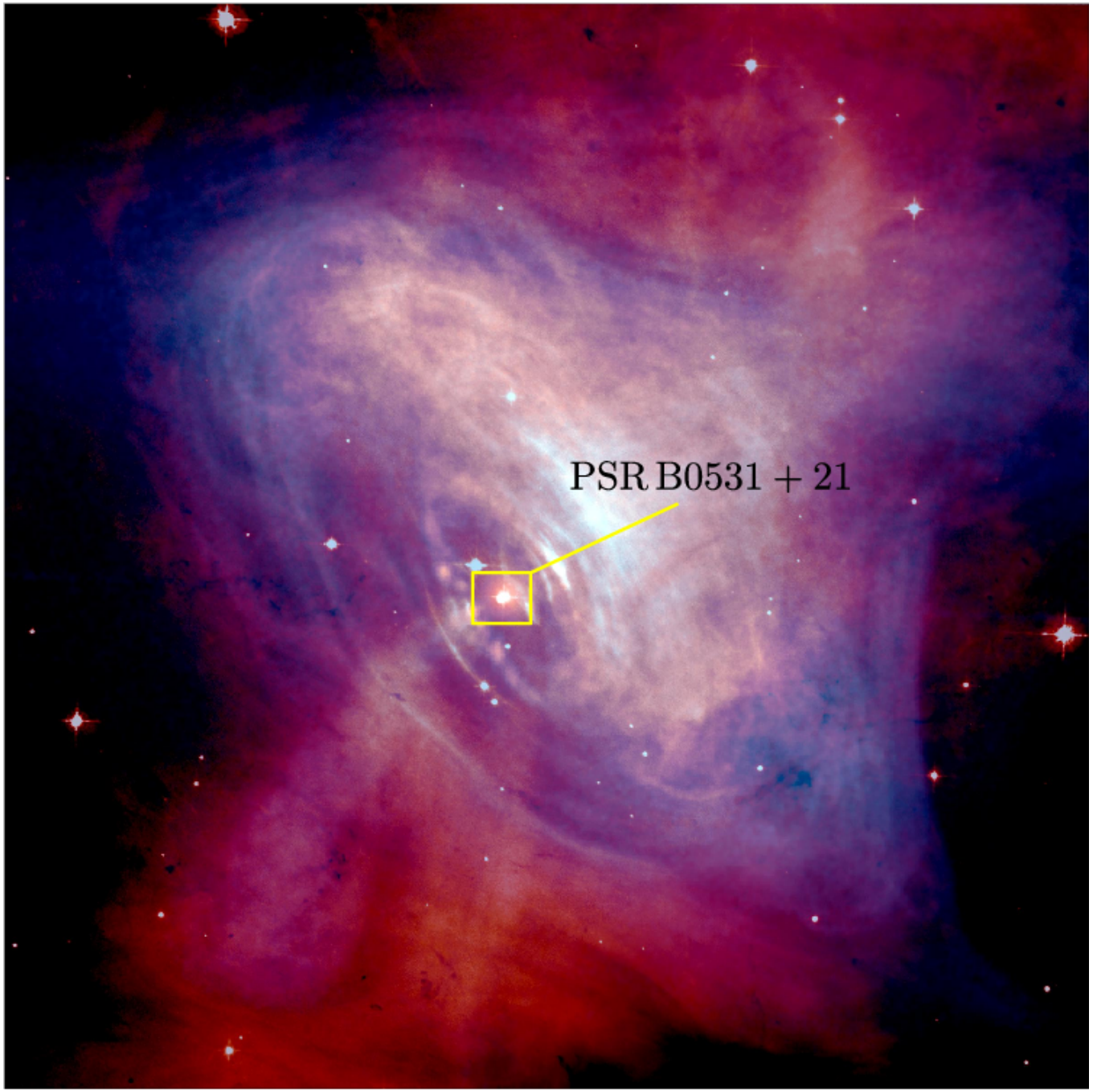
PSR B0531 + 21

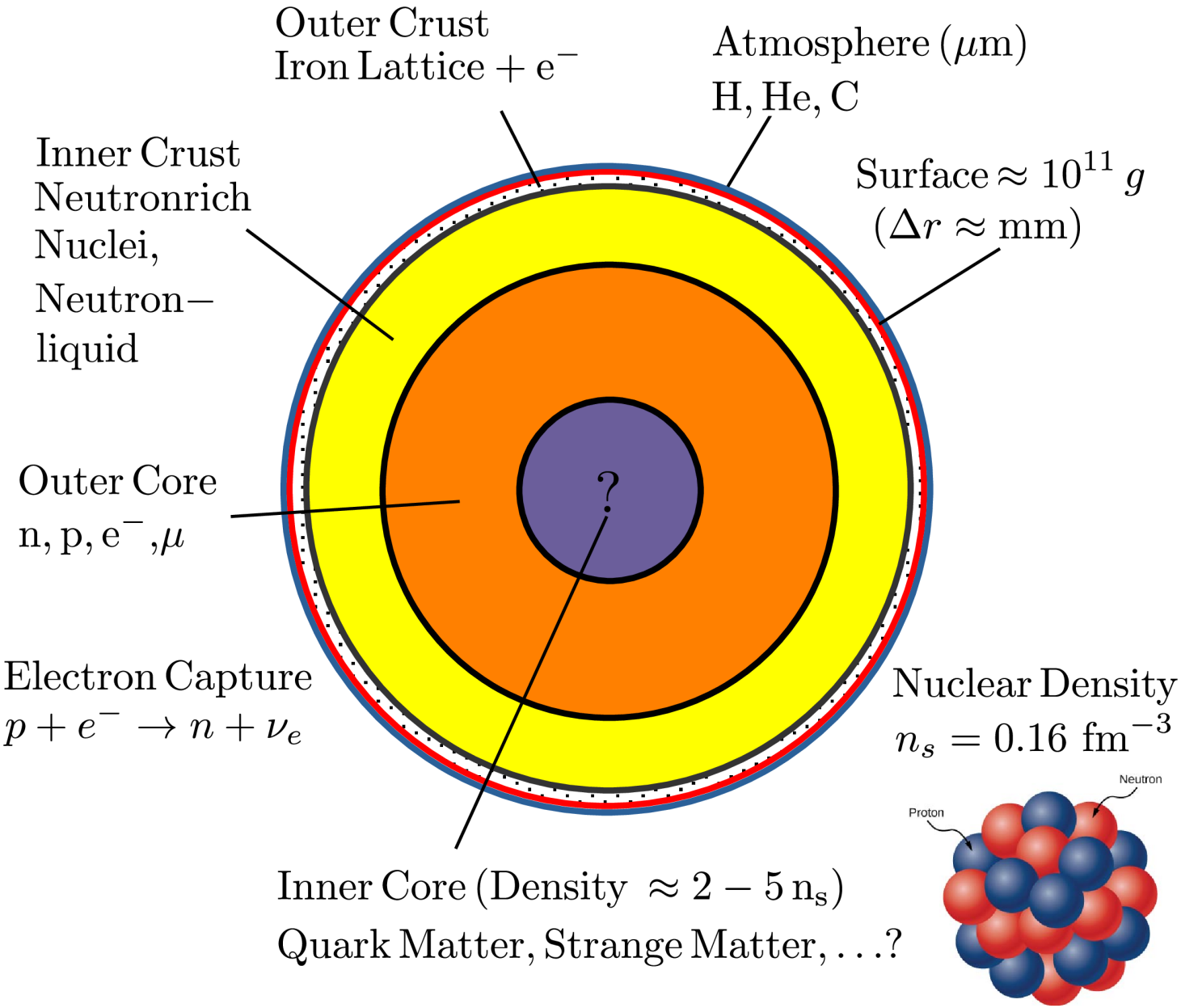
Outer Crust
Iron Lattice + e$^-$
Atmosphere (μm)
H, He, C
Inner Crust
Neutronrich
Nuclei,
Neutron−
liquid
Surface $\approx 10^{11}$ g
($\Delta r \approx$ mm)
Outer Core
n, p, e$^-$,μ
?
Electron Capture
$p + e^- \rightarrow n + \nu_e$
Nuclear Density
$n_s = 0.16$ fm^{-3}
Neutron
Proton
Inner Core (Density $\approx 2 - 5$ n$_s$)
Quark Matter, Strange Matter, . . .?

Density Profile

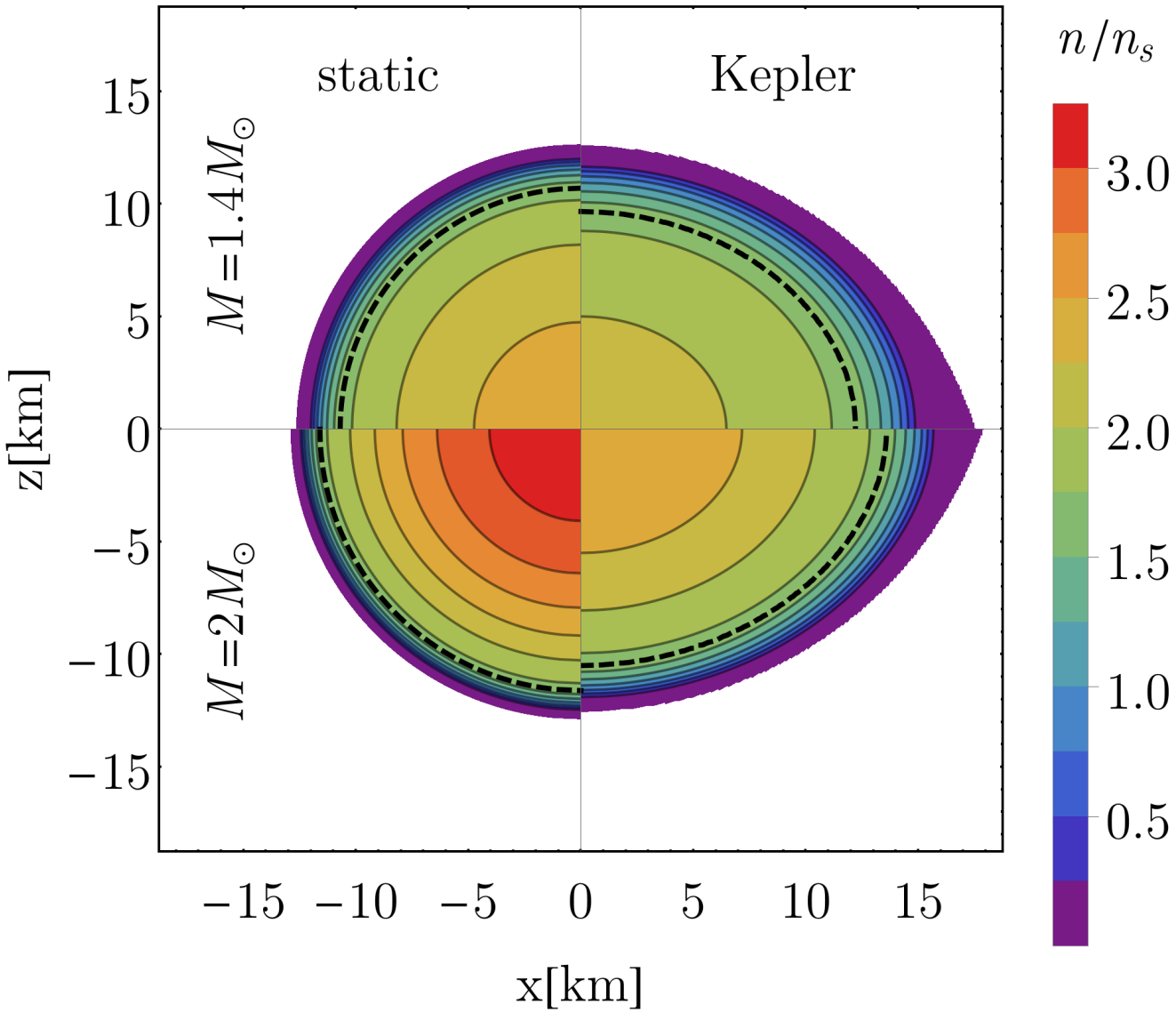

Demircik, CE, Järvinen 2009.10731 (ApJL)

Equation of State

Relates properties of dense matter to properties of neutron stars.

$$p = p(e, \ldots) \xrightarrow{\text{Einstein Eq.}} M(R)$$

Constrained by theory and neutron star observations:

- Causality & thermodynamic stability: $0 < c_s^2 = \frac{\mathrm{d}p}{\mathrm{d}e} < 1$
- Direct mass and radius measurements: $M_{\mathrm{TOV}} \gtrsim 2\,M_\odot$, $11\,\mathrm{km} \lesssim R \lesssim 14\,\mathrm{km}$
- First GW detection from a BNS merger GW170817: $\tilde{\Lambda} \lesssim 720$

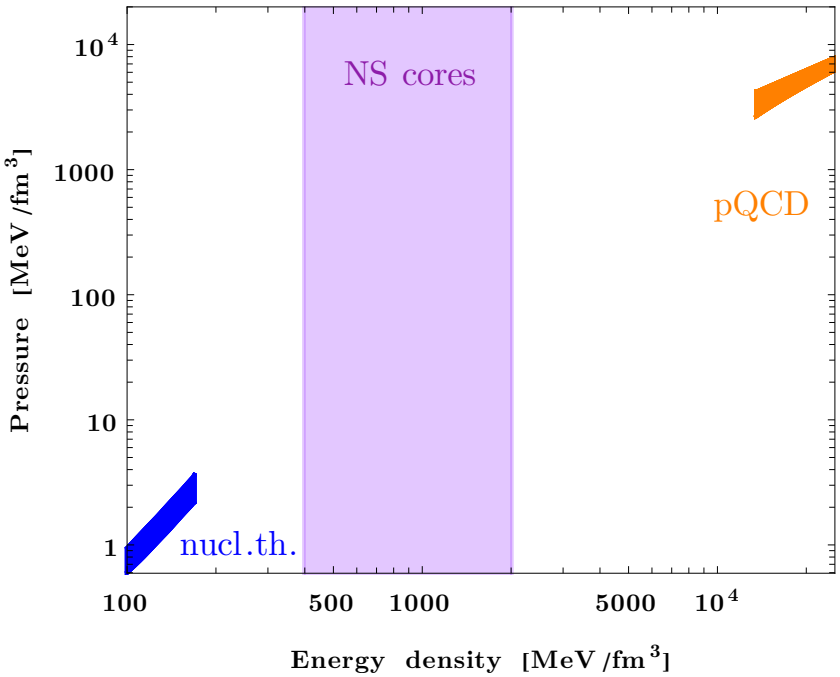

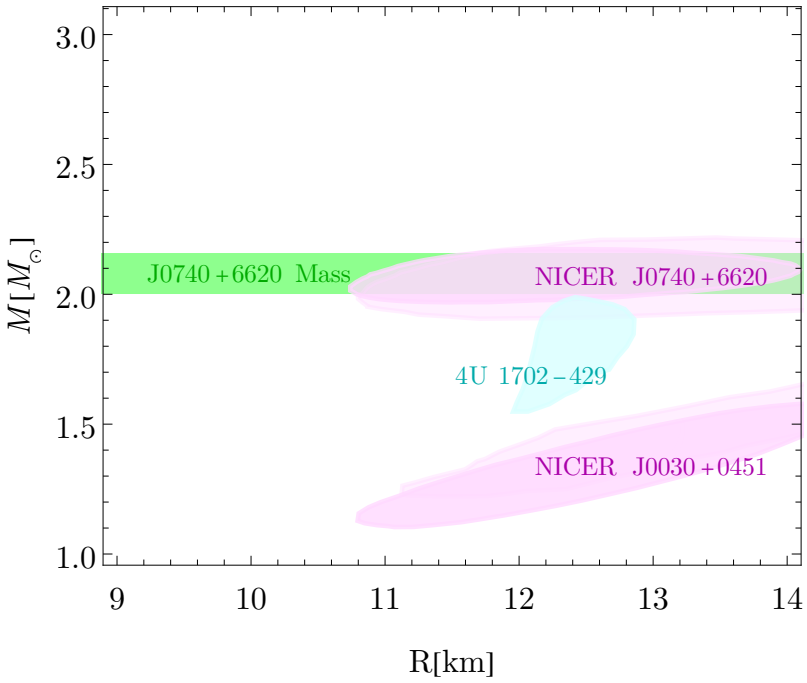

Equation of State

Relates properties of dense matter to properties of neutron stars.

$$p = p(e, \ldots) \xrightarrow{\text{Einstein Eq.}} M(R)$$

Constrained by theory and neutron star observations:

- Causality & thermodynamic stability: $0 < c_s^2 = \frac{\mathrm{d}p}{\mathrm{d}e} < 1$
- Direct mass and radius measurements: $M_{\mathrm{TOV}} \gtrsim 2\,M_\odot$, $11\,\mathrm{km} \lesssim R \lesssim 14\,\mathrm{km}$
- First GW detection from a BNS merger GW170817: $\tilde{\Lambda} \lesssim 720$

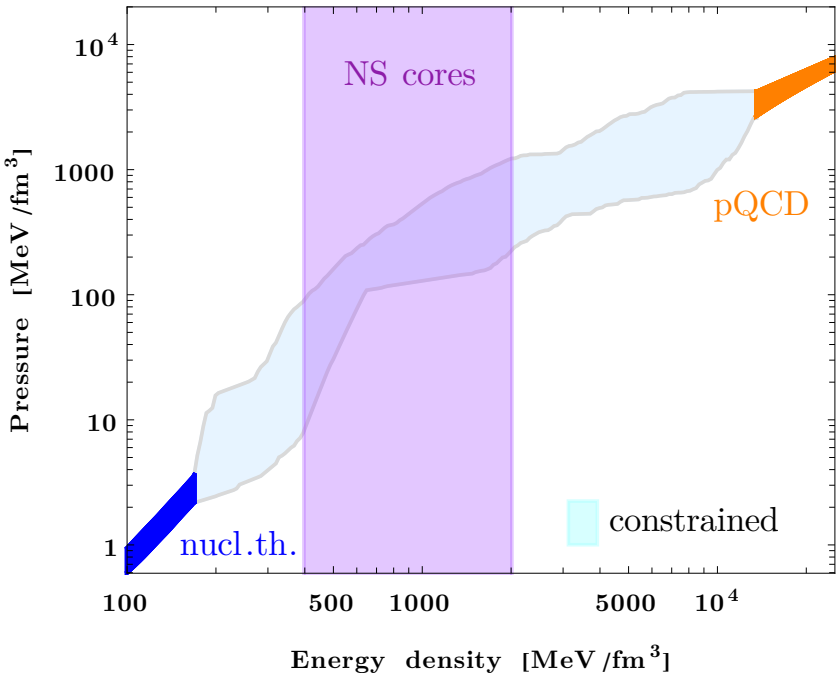

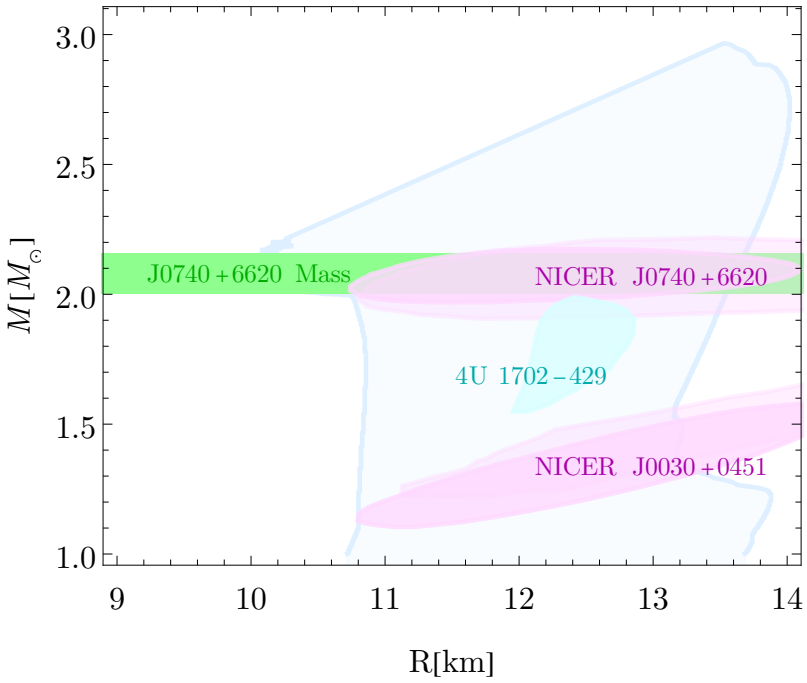

Agnostic Approach

- Impose boundary conditions from nuclear theory and perturbative QCD.
  Hebeler, Lattimer, Pethick, Schwenk 1303.4662 (ApJ);
  Fraga, Kurkela, Vuorinen 1311.5154 (ApJL)
- Connect with random, but causal and thermodynamically consistent EOS.

$$c_s^2(\mu)=\frac{\left(\mu_{i+1}-\mu\right)c_{s,i}^2+(\mu-\mu_i)c_{s,i+1}^2}{\mu_{i+1}-\mu_i}\,,\qquad n(\mu)=n_1\,e^{\int_{\mu_1}^{\mu}\frac{\mathrm{d}\mu'}{\mu' c_s^2(\mu')}}\,,\qquad p(\mu)=p_1+\int_{\mu_1}^{\mu}\mathrm{d}\mu' n(\mu')\,.$$

Annala, Gorda, Kurkela, Nättilä, Vuorinen 1903.09121 (Nature Physics)

- Constrain with pulsar and binary neutron star observations.

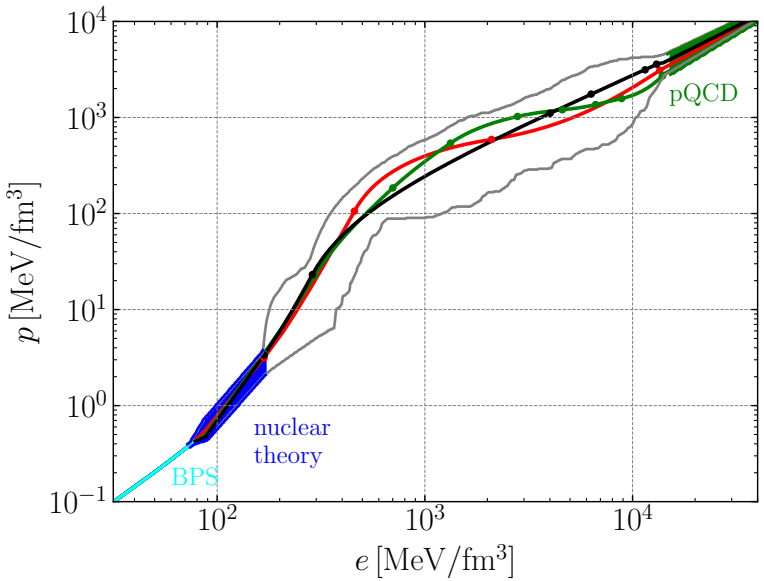

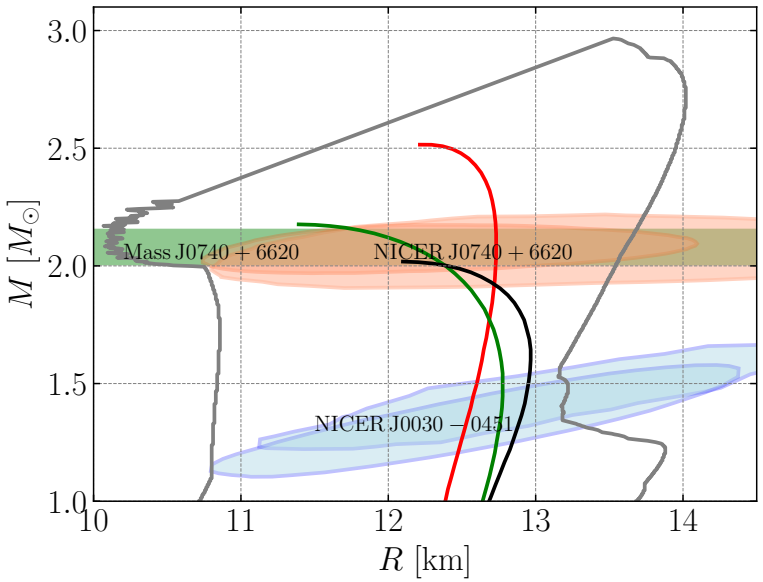

Lots of recent work:
. . . ; Annala, Gorda, Kurkela, Nättilä, Vuorinen 2105.05132 (PRX);
Komoltsev, Kurkela 2111.05350 (PRL); Altiparmak, CE, Rezzolla 2203.14974 (ApJL);
Gorda, Komoltsev, Kurkela 2204.11877; CE, Rezzolla 2207.04417 (ApJL); . . .

Sampling the EOS

- Statistics of millions of EOS models that pass theory+astro constraints.
- Mass bound of generic (sub-conformal) models: $M_{\rm TOV} < 3\,(2.1)\,M_\odot$.
- Radius estimates (+ error bars) for typical stars:

$$R_{1.4} = 12.42^{+0.52}_{-0.99}\,\mathrm{km}\,,\; R_{2.0} = 12.11^{+1.11}_{-1.23}\,\mathrm{km}\,(95\%\,\mathrm{confidence})\,. \qquad (1)$$

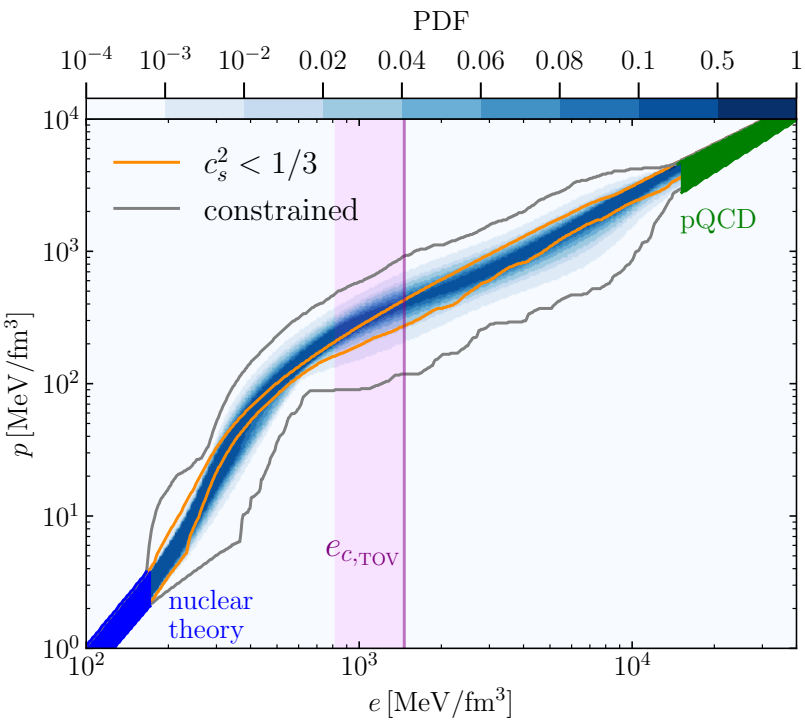

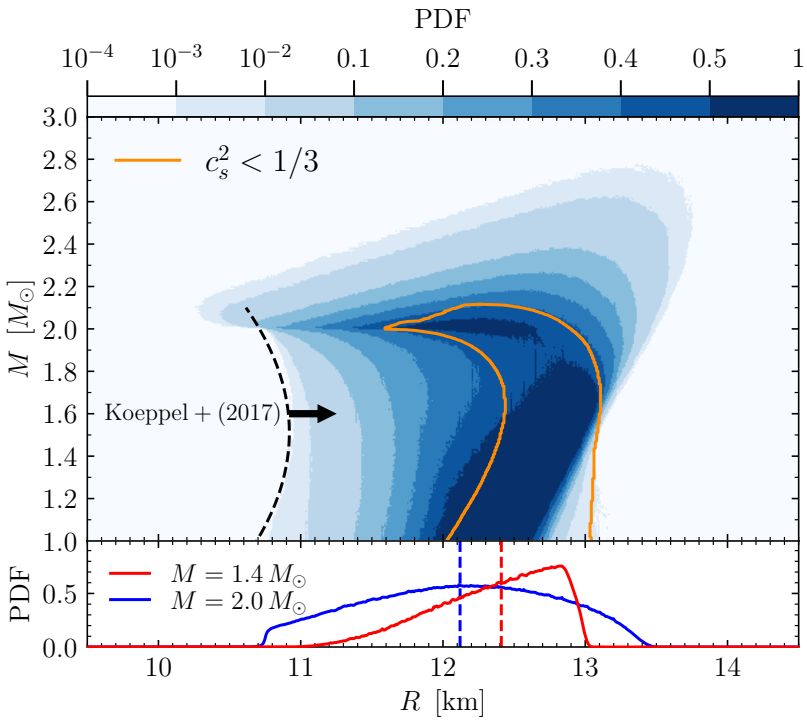

Altiparmak, CE, Rezzolla 2203.14974 (ApJL)

Sound Speed in Dense Matter

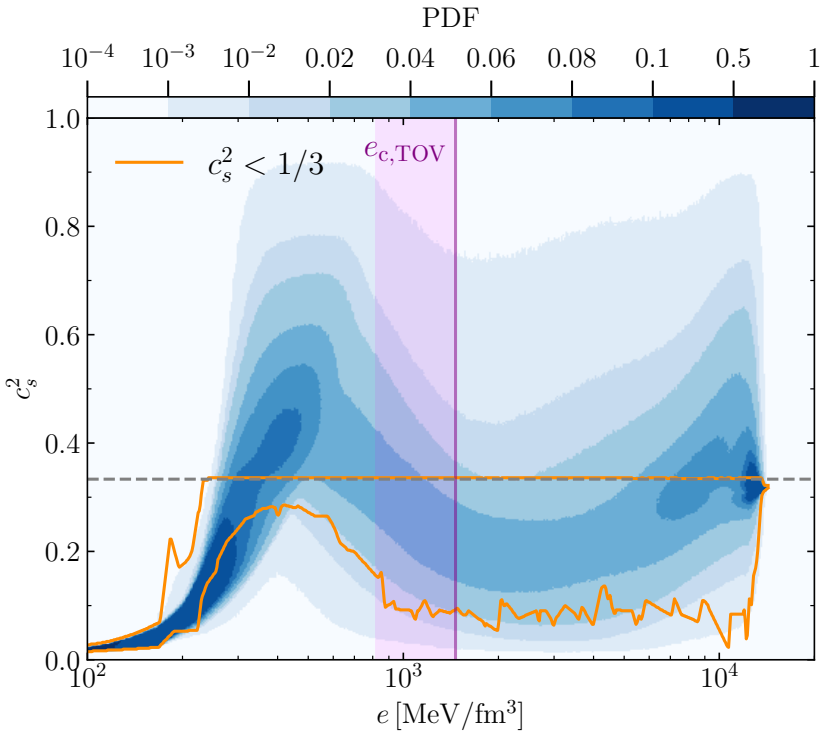

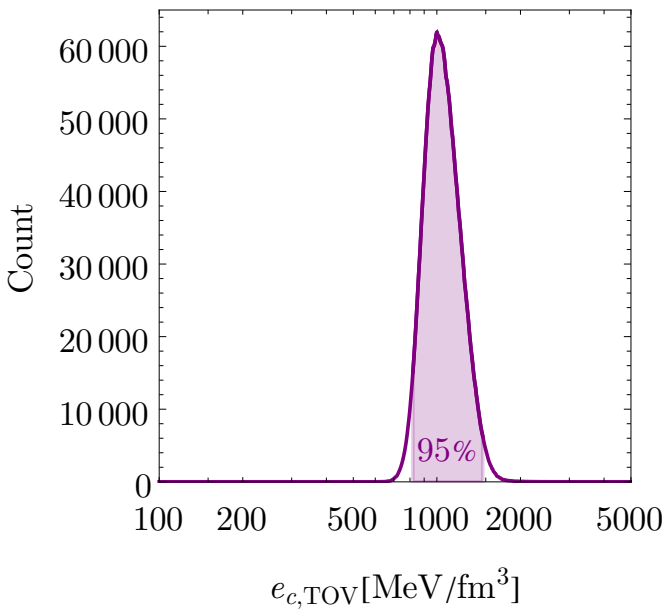

- Local maximum $c_s^2 > 1/3$ below maximal central densities of TOV stars

$$e_{c,\mathrm{TOV}} = 1064^{+399}_{-244}\,\mathrm{MeV/fm^3}\ (95\%\,\mathrm{confidence})\,.$$

- $c_s^2 \leqslant 1/3$ at all densities possible, but only a small fraction (0.03%).
- Lower bound $c_s^2 \gtrsim 0.2$ of sub-conformal models around $e \approx 400\,\mathrm{MeV/fm^3}$.
- Monotonic sound speed is impossible: $M_{\mathrm{TOV}}^{\max} < 2\,M_\odot$.

Altiparmak, CE, Rezzolla 2203.14974 (ApJL)

Speed of Sound inside Neutron Stars?

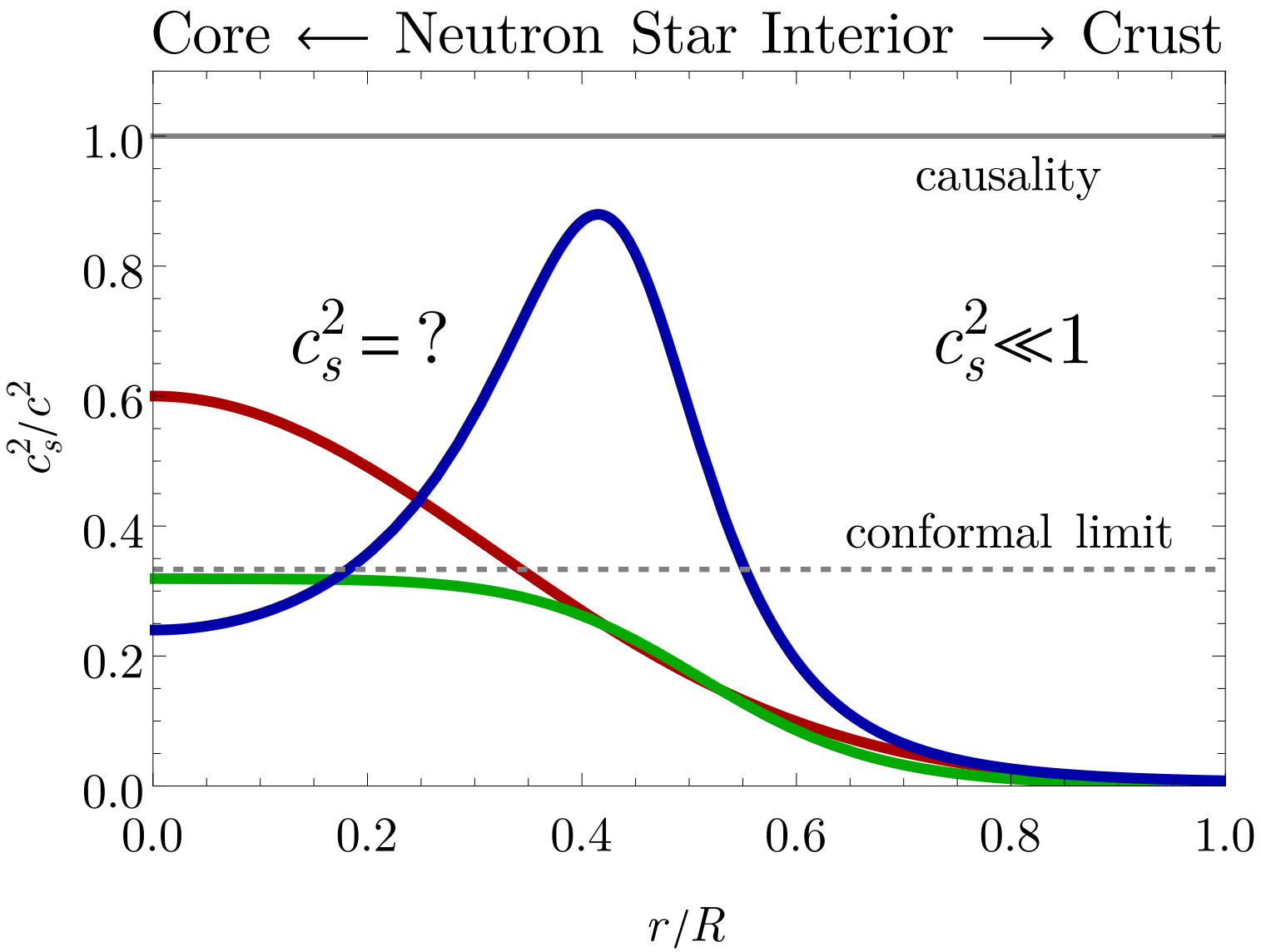

Speed of Sound inside Neutron Stars

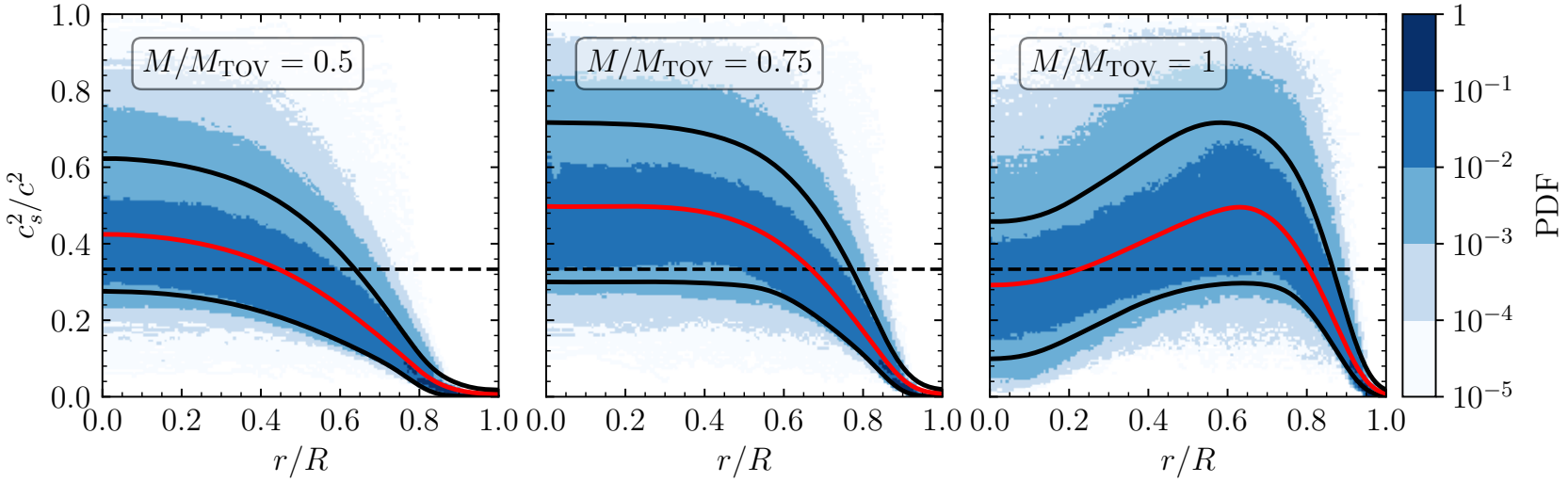

Median (red) and 95% intervals (black) can be accurately described by

$$c_s^2(x) = \left(\alpha e^{\beta x^2} + \gamma e^{\delta (x-\epsilon)^2}\right)\left[1 - \tanh\left(\zeta x - \eta\right)\right] , \quad x \equiv r/R \, .$$

- **Light Stars:** stiff core, soft outer layer.
- **Typical Stars:** large stiff core.
- **Massive Stars:** soft core, stiff outer layer.

CE, Rezzolla 2207.04417 (ApJL)

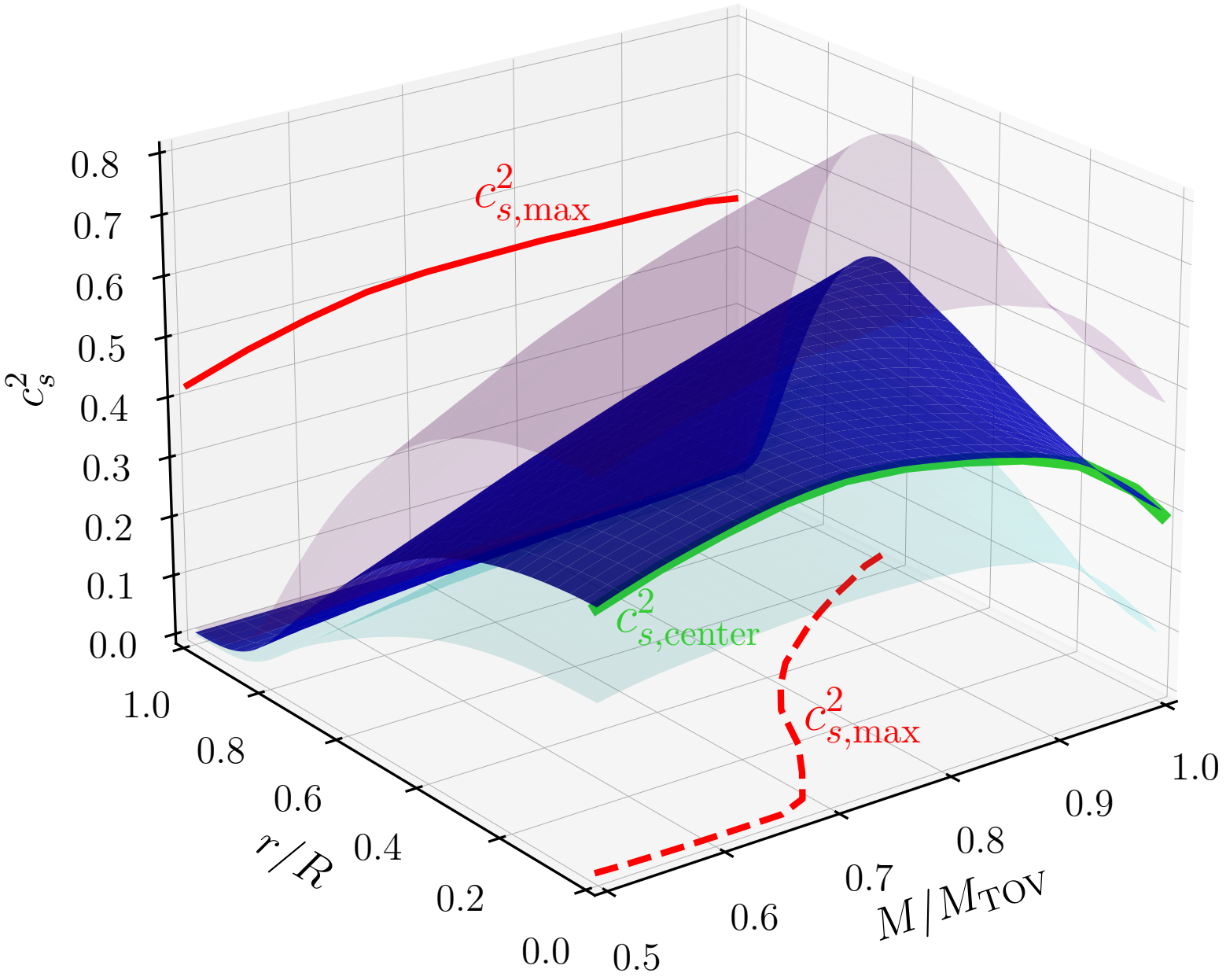

CE, Rezzolla 2207.04417 (ApJL)

Chirp Mass and Binary Tidal Deformability

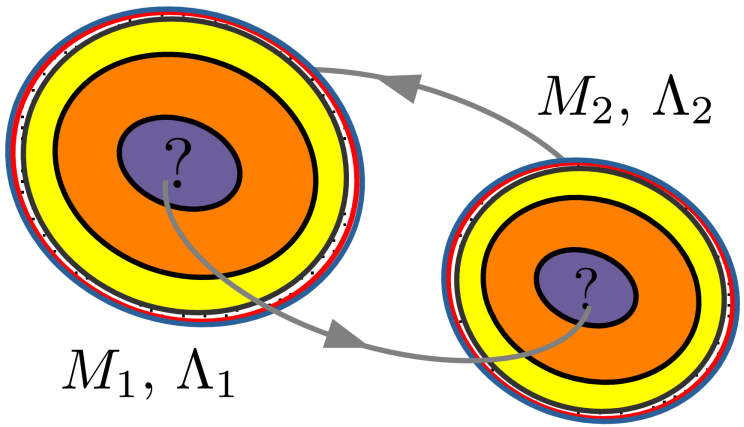

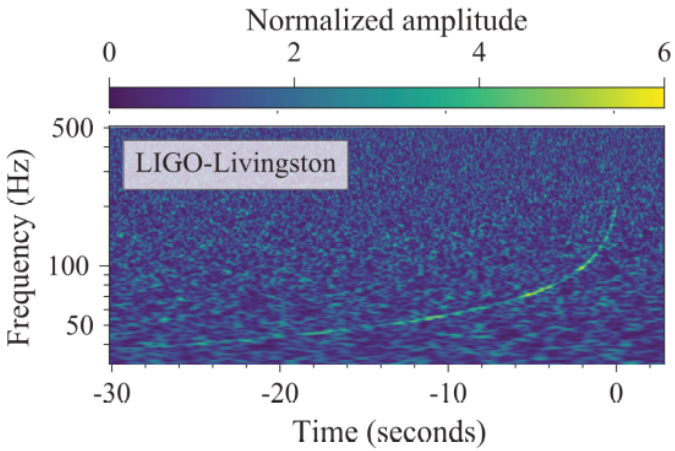

- Binary tidal deformability encodes EOS properties via Λ_i

$$\tilde{\Lambda} = \frac{16}{13}\frac{(12M_2 + M_1)\, M_1^4\Lambda_1 + (12M_1 + M_2)\, M_2^4\Lambda_2}{(M_1 + M_2)^5}\,, \quad \Lambda_i = \tfrac{2}{3}k_2\,(R_i/M_i)^5\,.$$

- Chirp mass can be extracted accurately from inspiral GW strain frequency

$$\mathcal{M}_{chirp} = \frac{(M_1 M_2)^{3/5}}{(M_1 + M_2)^{1/5}} = \left(\frac{5}{96}\pi^{-8/3} f^{-11/3}\dot{f}\right)^{3/5}\,.$$

- GW170817 only "good" event so far:

$$\mathcal{M}_{chirp} = 1.188^{+0.004}_{-0.002} M_\odot, \quad q = M_2/M_1 > 0.7, \quad \tilde{\Lambda} \lesssim 720\,.$$

LIGO/Virgo 1710.05832 (PRL), 1710.05834 (ApJL), 1805.11579 (PRX)

Binary Tidal Deformability

- More than 10^8 binary configurations with $M_{1,2} \in [0.5 M_\odot, M_{\rm TOV}]$.

$$\tilde{\Lambda}_{min(max)} = a + b\,\mathcal{M}_{chirp}^{c} \longrightarrow \tilde{\Lambda}_{1.186} = 485^{+225}_{-211}\,,$$

$$a = -50(-20),\ b = 500(1800),\ c = -4.5(-5.0)\,.$$

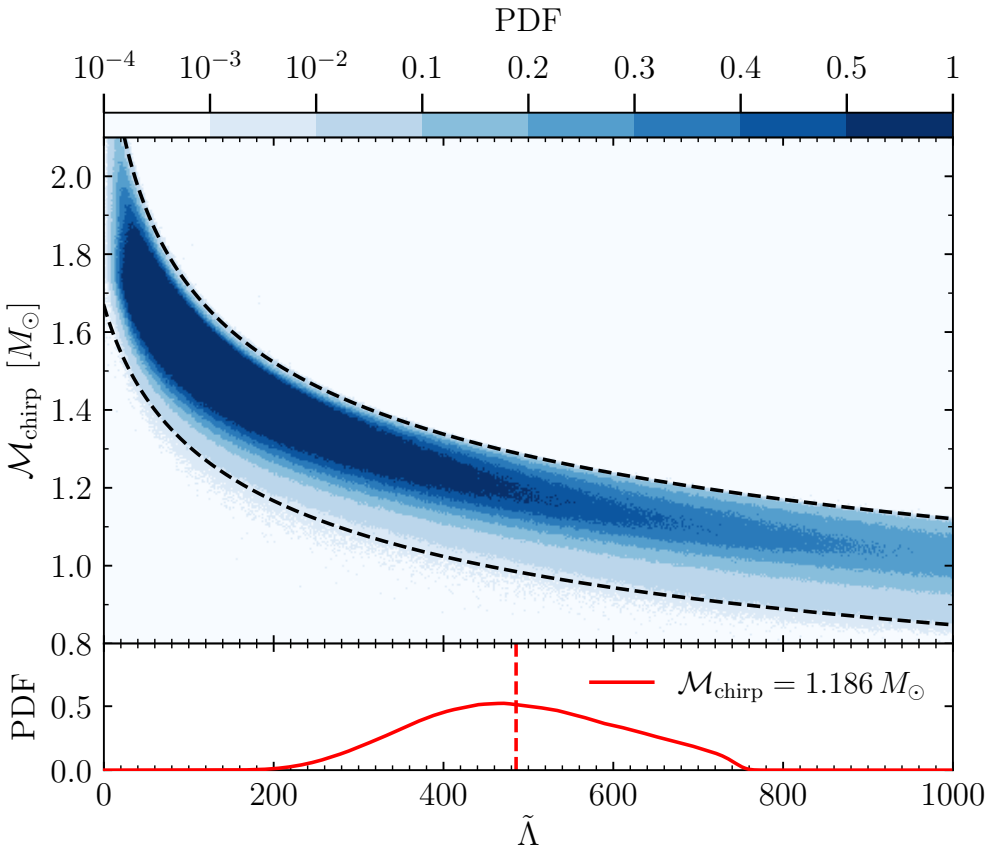

Altiparmak, CE, Rezzolla 2203.14974 (ApJL)

see also: Zhao, Lattimer 1808.02858 (PRD)

Black-Widow Binary Pulsar PSR J0952-0607

- Most massive NS known: $M = 2.35 \pm 0.17\, M_\odot$, but large uncertainties!

  Romani, Kandel, Filippenko, Brink, Zheng 2207.05124 (ApJL)

  also: PSR J2215+5135 ($M = 2.27^{+0.17}_{-0.15}\, M_\odot$) Linares, Shahbaz, Casares 1805.08799 (ApJ)
- Large mass constraints dominate over radius constraints by NICER.

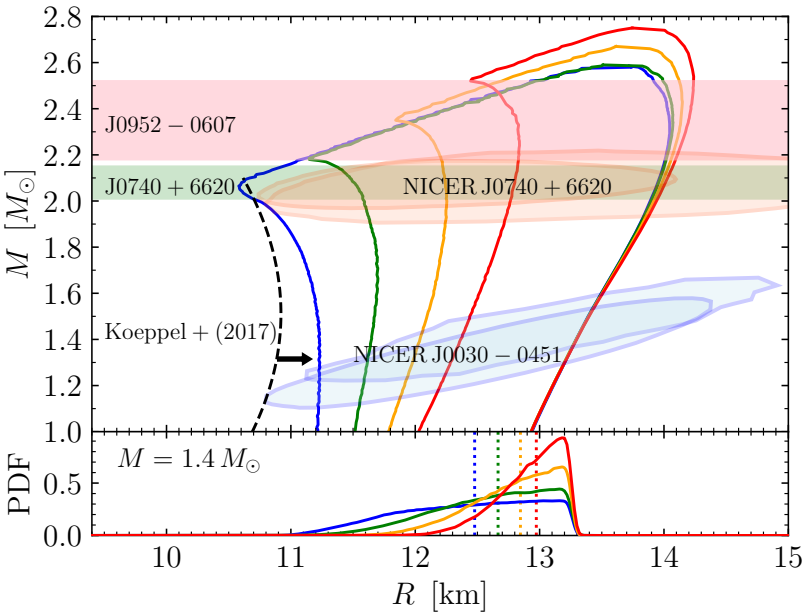

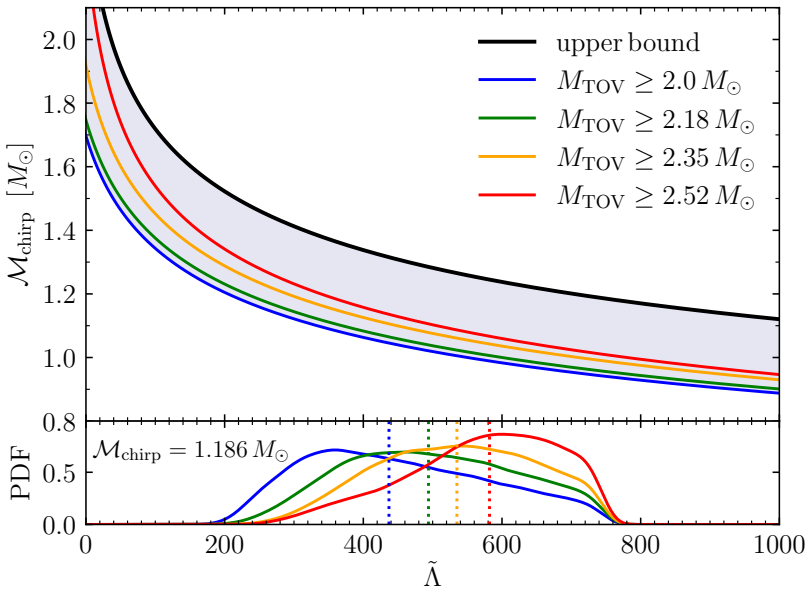

$M_{\rm TOV}\ [M_\odot]$	a	b	c
$\geqslant 2.00$	-50	600	4.7
$\geqslant 2.18$	-45	650	4.6
$\geqslant 2.35$	-40	750	4.5
$\geqslant 2.52$	-20	800	4.4

CE, Rezzolla 2209.08101 (MNRAS)

Sound Speed and Conformal Anomaly

$$\Delta := \frac{1}{3}\frac{g_{\mu\nu}T^{\mu\nu}}{e} = \frac{1}{3} - \frac{p}{e}\,, \qquad -\frac{2}{3} \leqslant \Delta \leqslant \frac{1}{3}\,.$$

Fujimoto, Fukushima, McLerran, Praszalowicz 2207.06753 (PRL)

Marczenko, McLerran, Redlich, Sasaki 2207.13059

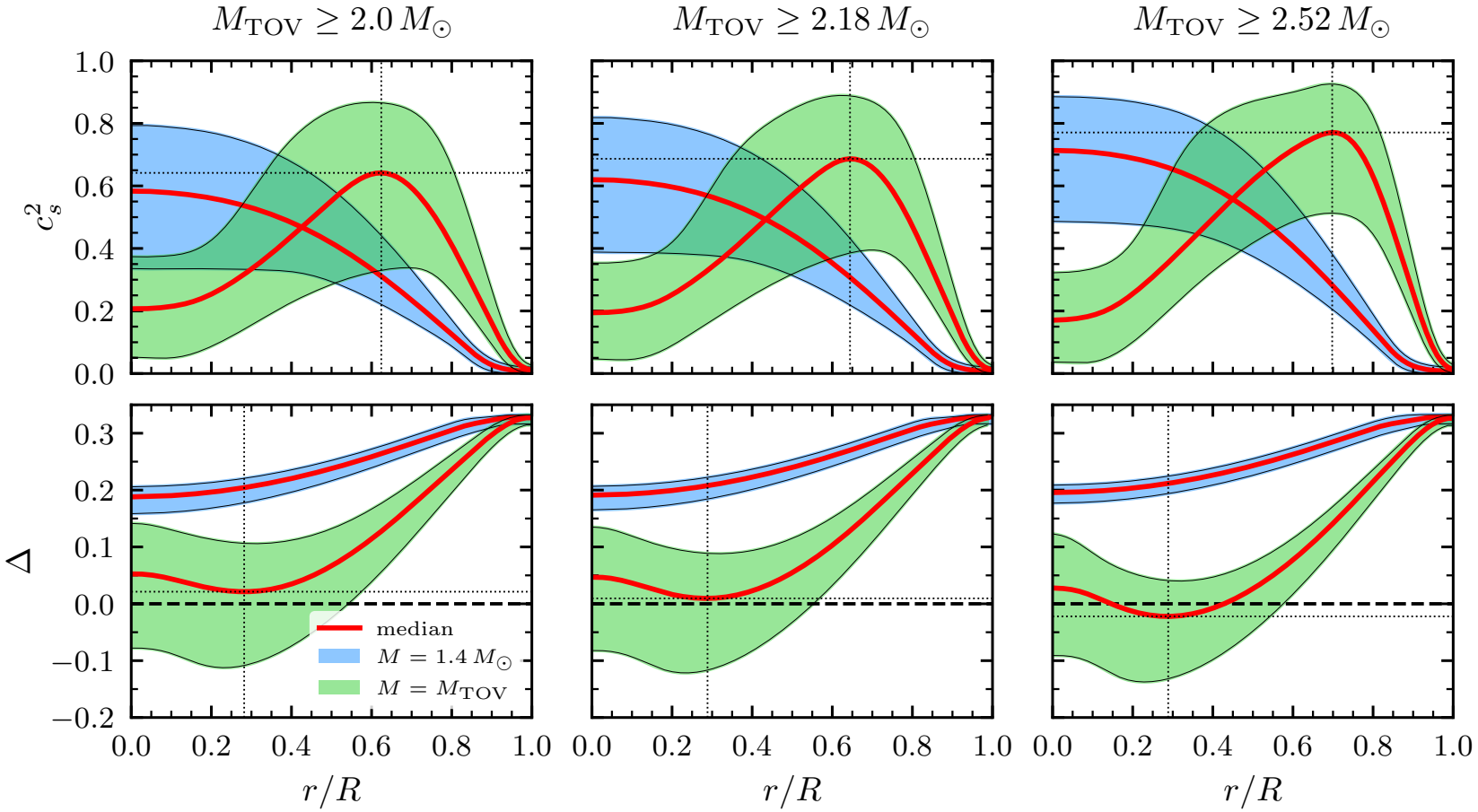

CE, Rezzolla 2209.08101 (MNRAS)

Quasi-Universality of the Pressure Profile

$$\frac{p(x)}{p_c} = e^{\alpha x^2} + e^{\alpha}\frac{\cos\beta x - 1}{\cos\beta - 1}\,, \quad x \equiv r/R\,.$$

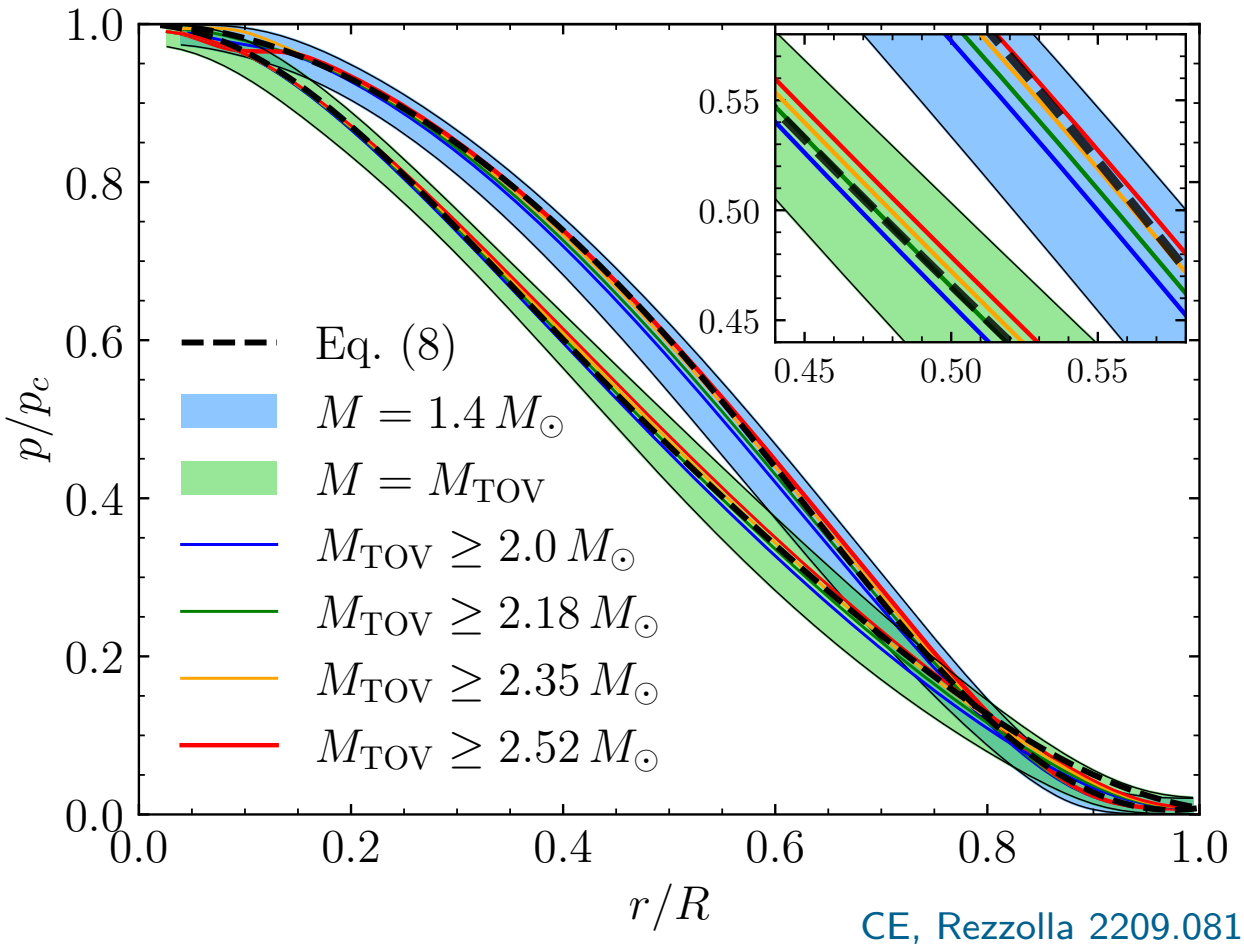

CE, Rezzolla 2209.08101 (MNRAS)

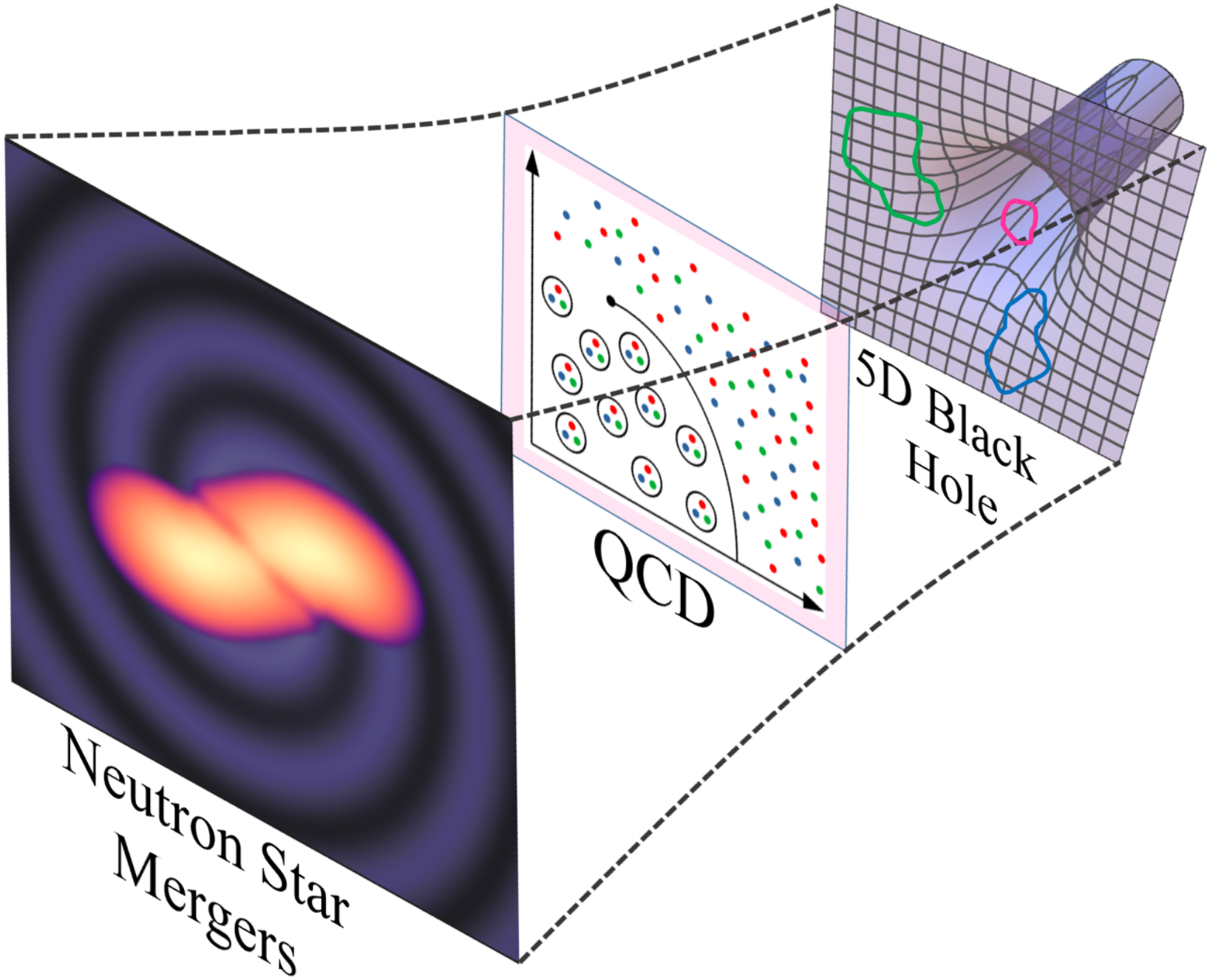
Neutron Star
Mergers
QCD
5D Black
Hole

A Holographic Approach to Dense QCD Matter

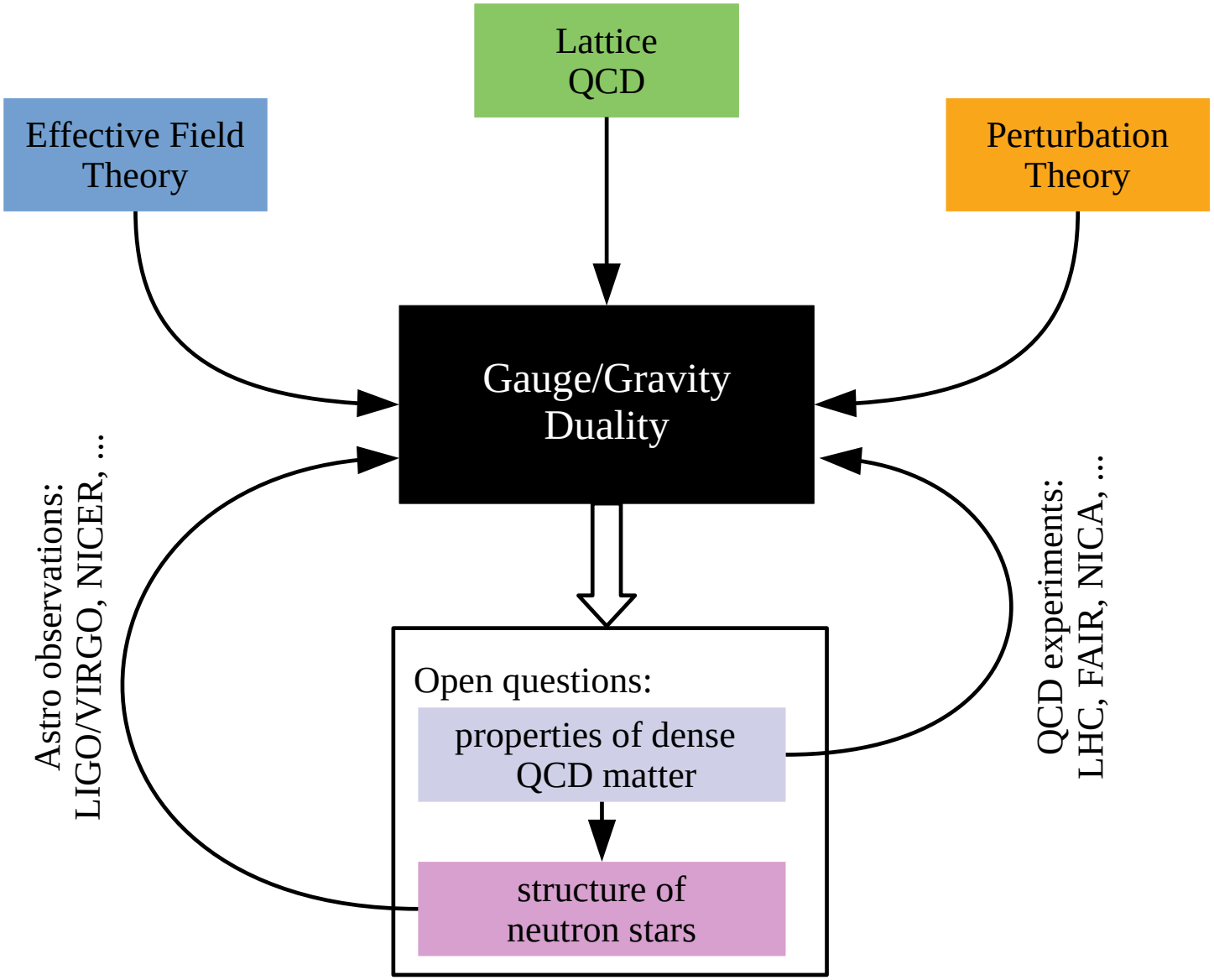

Applications of Holography to Neutron Stars

- Early attempts with D3-D7 hybrid EOS models.
  Hoyos, Fernandez, Jokela, Vuorinen 1603.02943 (PRL);
  Annala, CE, Hoyos, Fernandez, Jokela, Vuorinen 1711.06244 (JHEP)
- First BNS merger simulations with input from holography.
  CE, Järvinen, Nijs, van der Schee 1908.03213 (PRD)
- Rapidly rotating stars (GW190814) with V-QCD model.
  Demircik,CE, Järvinen 2009.10731 (ApJL)
- Superconducting holographic quark matter in compact stars.
  Bitaghsir Fadafan, Cruz Rojas, Evans 2009.14079 (PRD)
- Neutron stars with superconducting QCD matter from 6D holography.
  Ghoroku, Kashiwa, Nakano, Tachibana, Toyoda 2107.14450 (PRD)
- Realistic neutron stars from Witten-Sakai-Sugimoto (WSS) model.
  Kovensky, Poole, Schmitt 2111.03374 (PRD)
- Merger simulations with holographic hard-wall model.
  Bartolini, Gudnason, Leutgeb, Rebhan 2202.12845 (PRD)
- More references on holographic EOS modelling in two review articles.
  Järvinen 2205.05691 (EPJC), Hoyos, Jokela,Vuorinen 2112.08422 (Prog.Part.Nucl.Phys.)

Holographic Veneziano QCD

Holographic bottom-up model for QCD with many parameters that are tuned to mimic QCD and that are constrained by lattice QCD data.

Järvinen, Kiritsis 1112.1261 (JHEP)

Gluons: Improved holographic QCD (Einstein-dilaton gravity)

$$S_{\rm g} = N_c^2 M^3 \int d^5x \sqrt{-g} \left[R - \tfrac{4}{3} \tfrac{(\partial\lambda)^2}{\lambda^2} + V_g(\lambda) \right]$$

$\lambda \equiv e^{\phi} \leftrightarrow \mathrm{Tr} F^2$ sources the 't Hooft coupling in YM theory

Gürsoy, Kiritsis 0707.1324 (JHEP); Gürsoy, Kiritsis, Nitti 0707.1349 (JHEP)

Quarks: Tachyonic Dirac-Born-Infeld (DBI) action

$$S_{\rm f} = -N_f N_c M^3 \int d^5x V_{f0}(\lambda) e^{-\tau^2} \sqrt{-\det\left[g_{ab} + \kappa(\lambda)\partial_a\tau\partial_b\tau + w(\lambda)F_{ab}\right]}$$

$$F_{rt} = \Phi'(r)\,, \quad \Phi(0) = \mu\,,$$

tachyon $\tau \leftrightarrow \bar{q}q$ controls chiral symmetry breaking.

Bigazzi et al. 0505140 (JHEP); Casero et al. 0702155 (Nucl.Phys.B)

Baryons: homogeneous solution of non-Abelian DBI + Cern–Simons action.

Ishii, Järvinen, Nijs 1903.06169 (JHEP)

Veneziano limit: $N_c \to \infty$ and $N_f \to \infty$ with $N_f/N_c = \mathcal{O}(1)$ fixed

Järvinen, Kiritsis 1112.1261 (JHEP)

Cold V-QCD Hybrid Equation of State

- Computing neutron star properties requires EOS at low and high densities.
- Homogeneous approximation for V-QCD baryons not reliable at low densities: use results from nuclear theory to model the low density part.
- Hybrid EOSs: nuclear theory model at low densities + V-QCD model for dense baryonic and quark matter at large densities.

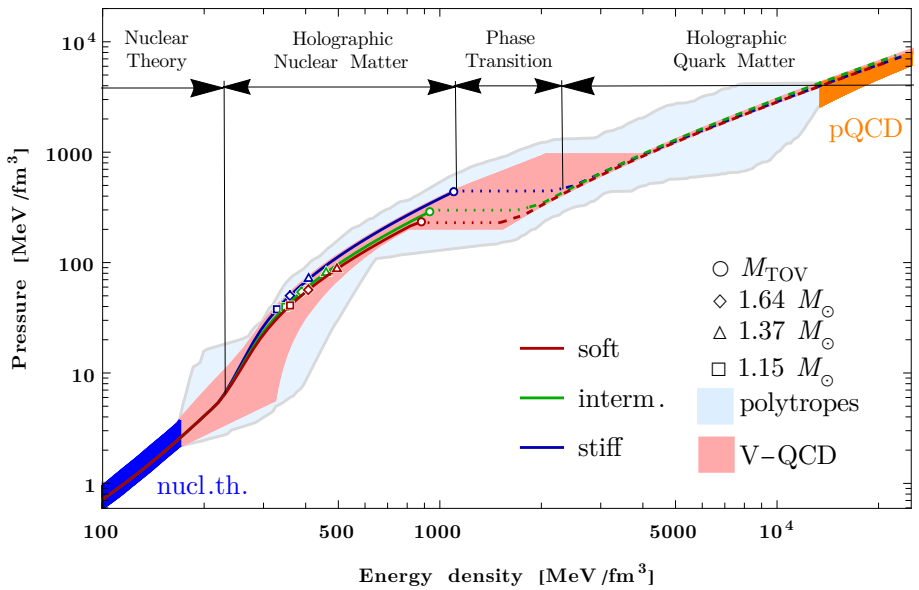

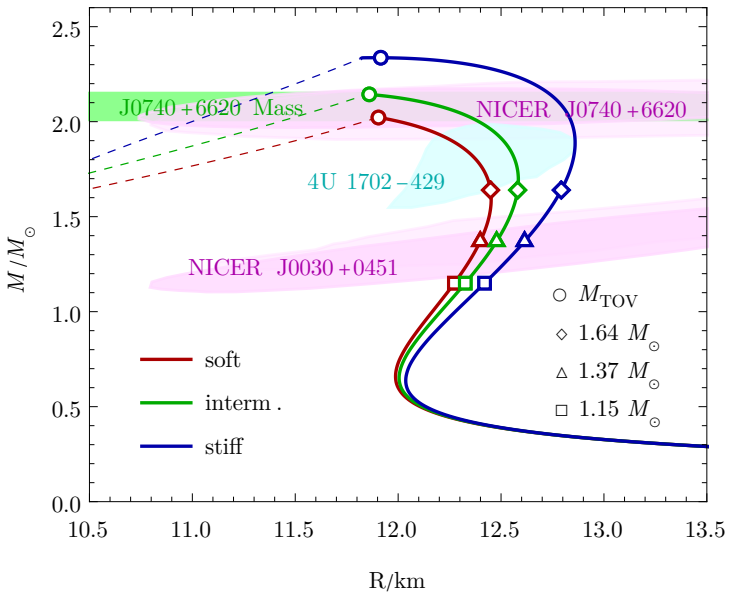

CE, Järvinen, Nijs, van der Schee 1908.03213 (PRD);
Jokela, Järvinen, Nijs, Remes 2006.01141 (JHEP); Demircik, CE, Järvinen 2112.12157 (PRX)

Hot V-QCD Hybrid Equation of State

- Low density part: Hemple-Schaffner-Bielich model (HS)DD2 + Particle Data Group (PDG) mesons. Hempel, Schaffner-Bielich 0911.4073 (Nucl.Phys.A); Zyla et al. (Particle Data Group 2020)
- (HS)DD2 too stiff around n_s, replace with APR model. Akmal, Pandharipande, Ravenhall 9804027 (PRC)
- Van der Waals construction to extend cold V-QCD baryons to finite-T. Vovchenko, Motornenko, Alba, Gorenstein, Satarov, Stoecker 1707.09215 (PRC)
- Mixed baryon and quark matter phase from Gibbs construction

$$X_{NM}(T, n_b^{(1)}, Y_q^{(1)}) = X_{QM}(T, n_b^{(2)}, Y_q^{(2)}), \quad X = \{p, \mu_b, \mu_{le}\}.$$

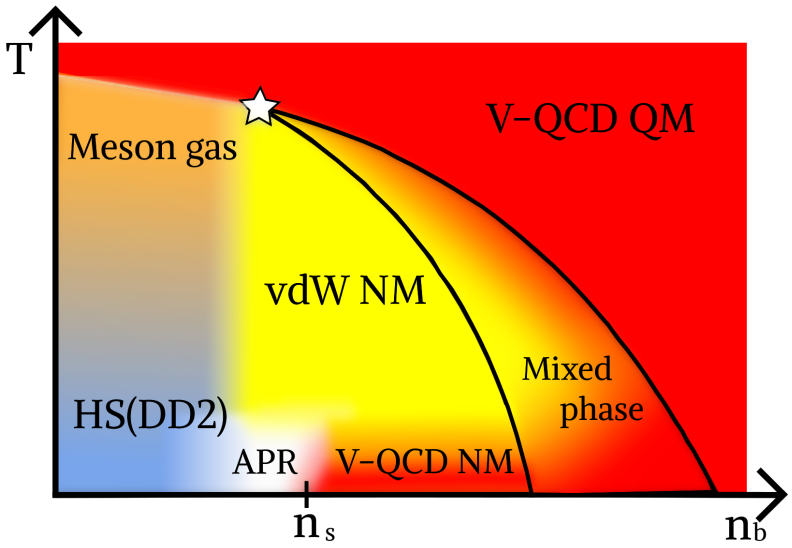

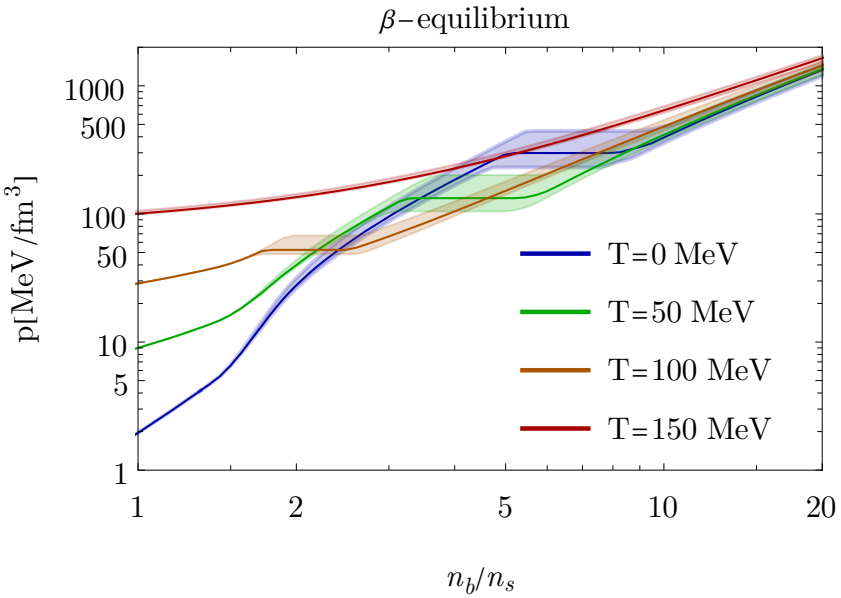

Demircik, CE, Järvinen 2112.12157 (PRX)

V-QCD Critical Point

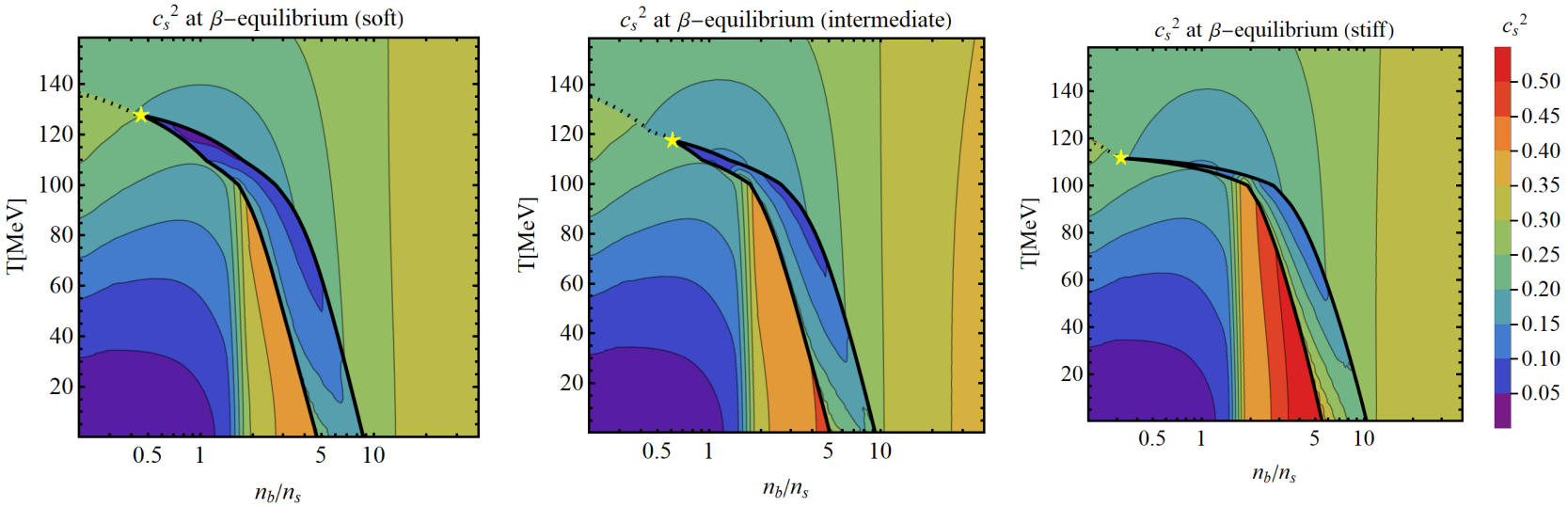

Estimates for the critical point:

$$110 \text{ MeV} \lesssim T_c \lesssim 130 \text{ MeV}$$
$$0.3\ n_s \lesssim n_c \lesssim 0.6\ n_s$$

model	$\frac{n_{bc}}{n_s}$	$\frac{\mu_{bc}}{\text{MeV}}$	$\frac{T_c}{\text{MeV}}$
soft	0.46	485	128
interm.	0.62	575	118
stiff	0.32	565	112

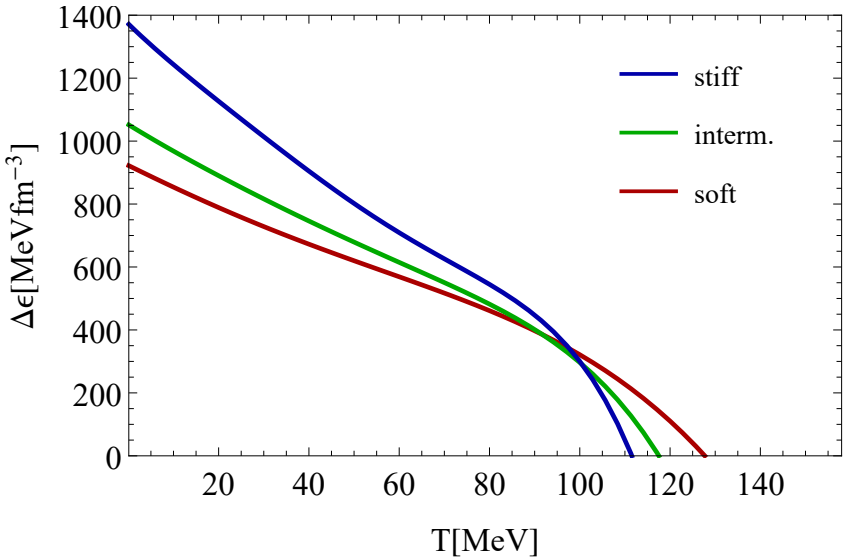

Demircik, CE, Järvinen 2112.12157 (PRX)

Binary Neutron Star Mergers

- Significant sources of gravitational radiation.
- Microscopic properties of dense matter encoded in GW and EM signal.
- Likely the origin of short gamma-ray bursts
- and of heavy elements like gold, platinum, uranium, ...

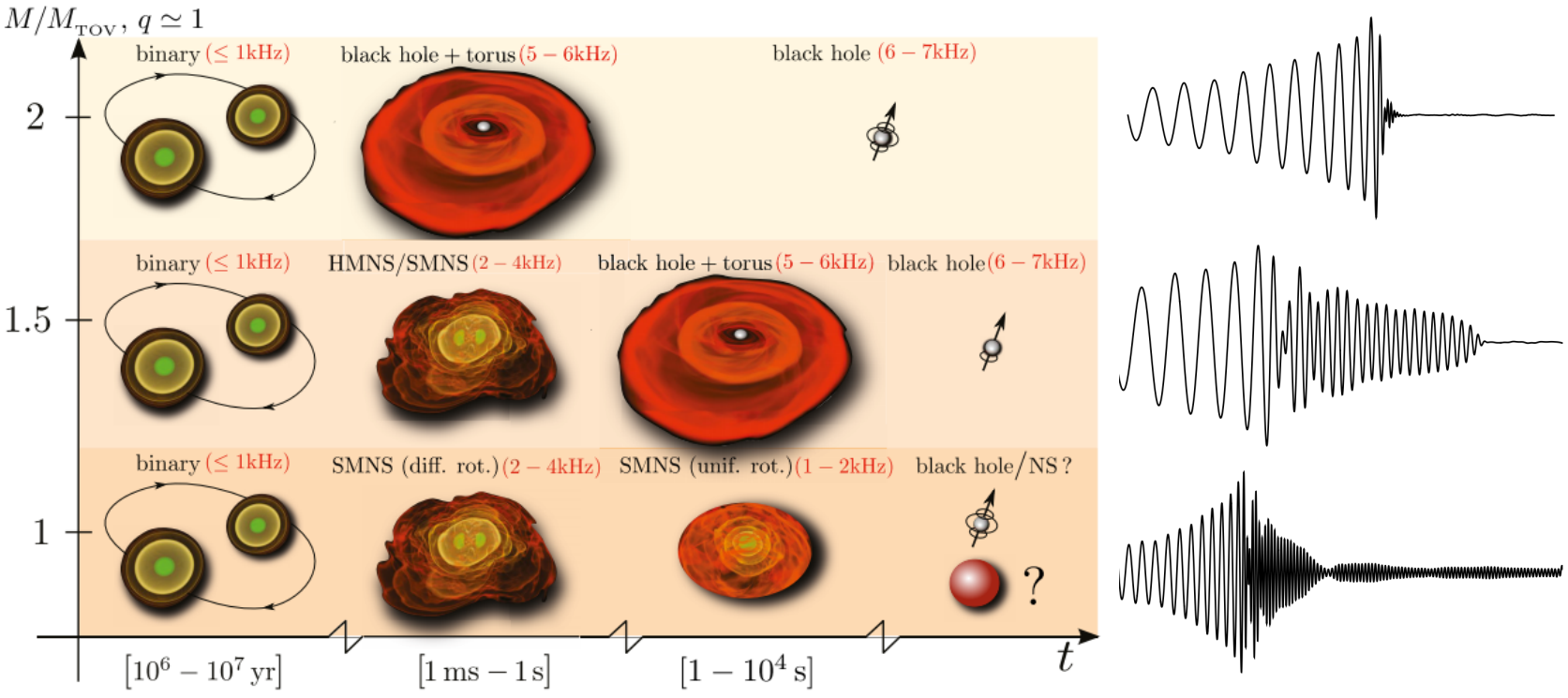

Picture: Baiotti, Rezzola 1607.03540 (Rept.Prog.Phys.)

Simulating Binary Neutron Star Mergers

Have to solve the 3+1D General Relativistic hydrodynamic equations:

$$R_{\mu\nu} - \frac{1}{2} R g_{\mu\nu} = 8\pi G_N T_{\mu\nu} \,, \quad \nabla_\mu T^{\mu\nu} = 0 \,, \quad \nabla_\mu J^\mu = 0 \,,$$

requires EOS $p = p(n_b, T, Y_e)$ as input and initial spacetime and fluid distribution that models a binary neutron star system.

- Powerful simulation tools developed in Frankfurt, mainly by a few renown and upcoming experts in numerical relativity:
  Elias Most, Carlo Musolino, Harry Ho-Yin Ng, Jens Papenfort, Samule Tootle, Konrad Topolski, Lukas Weih,...
- Spectral code Frankfurt University/Kadath (FUKA) for initial data.
  Papenfort, Tootle, Grandclement, Most, Rezzolla 2103.09911 (PRD)
- Frankfurt/Illinois (FIL) code for binary evolution with tabulated EOS.
  Most, Papenfort, Rezzolla 1907.10328 (MNRAS)
- Implemented in the Einstein Toolkit.
  http://einsteintoolkit.org

High-Performance Computing Center Stuttgart

- Project BNSMIC: 100+ million core-hours on HAWK.

Picture Copyright: Ben Derzian for HLRS

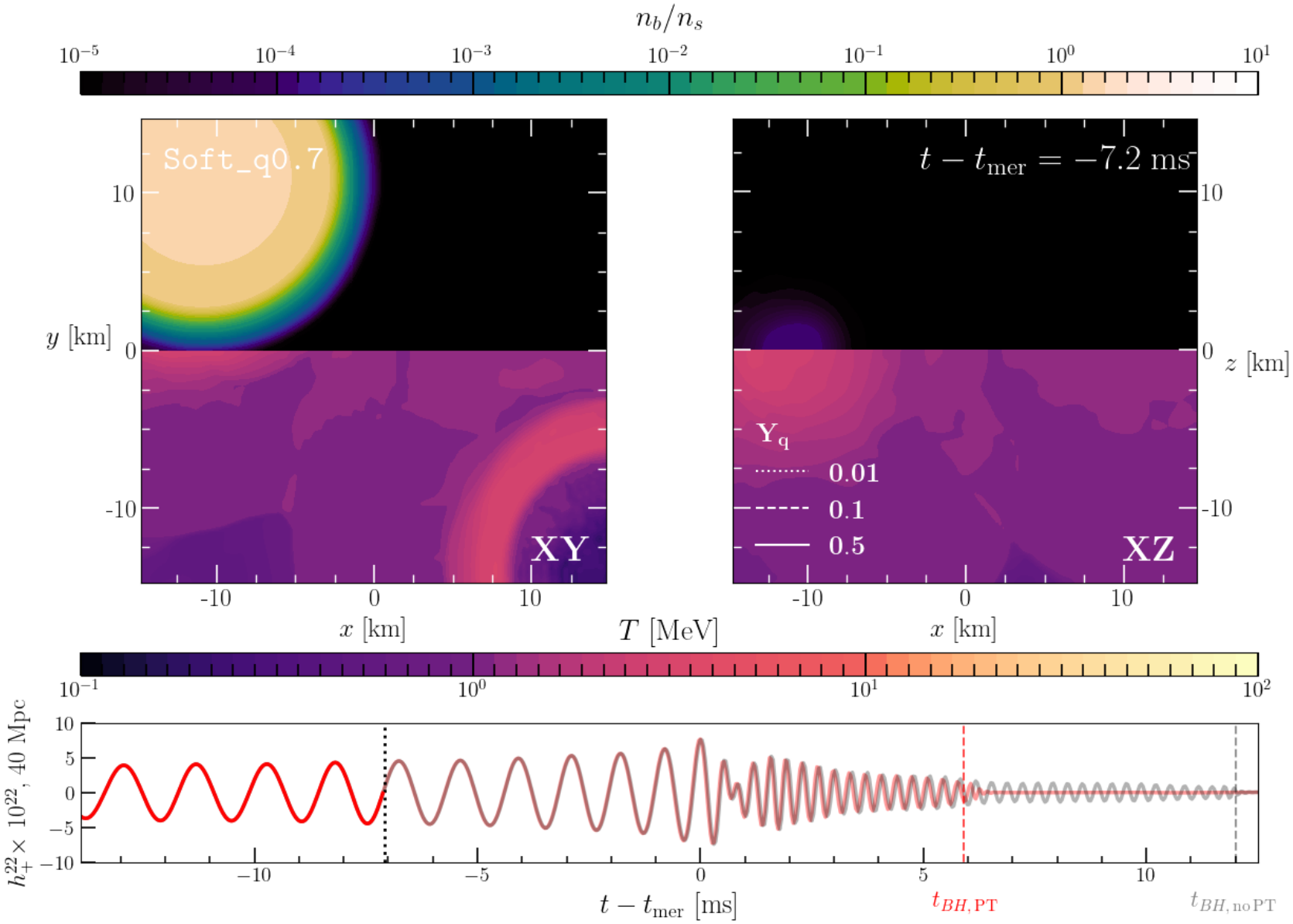

Movie by Konrad Topolski with data from 2205.05691 (SciPost).

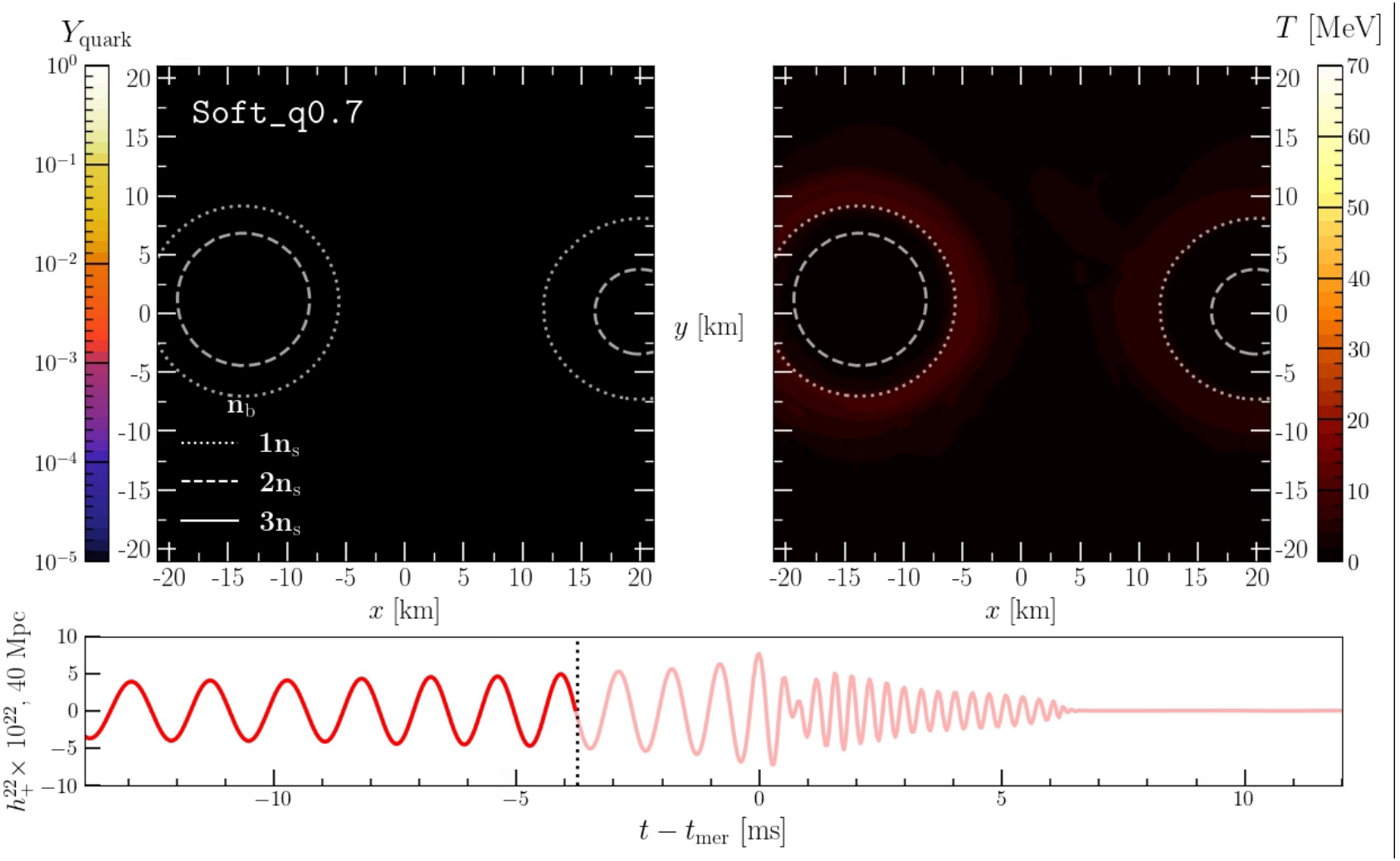

Movie by Konrad Topolski with data from 2205.05691 (SciPost).

Hot, Warm and Cold Quarks

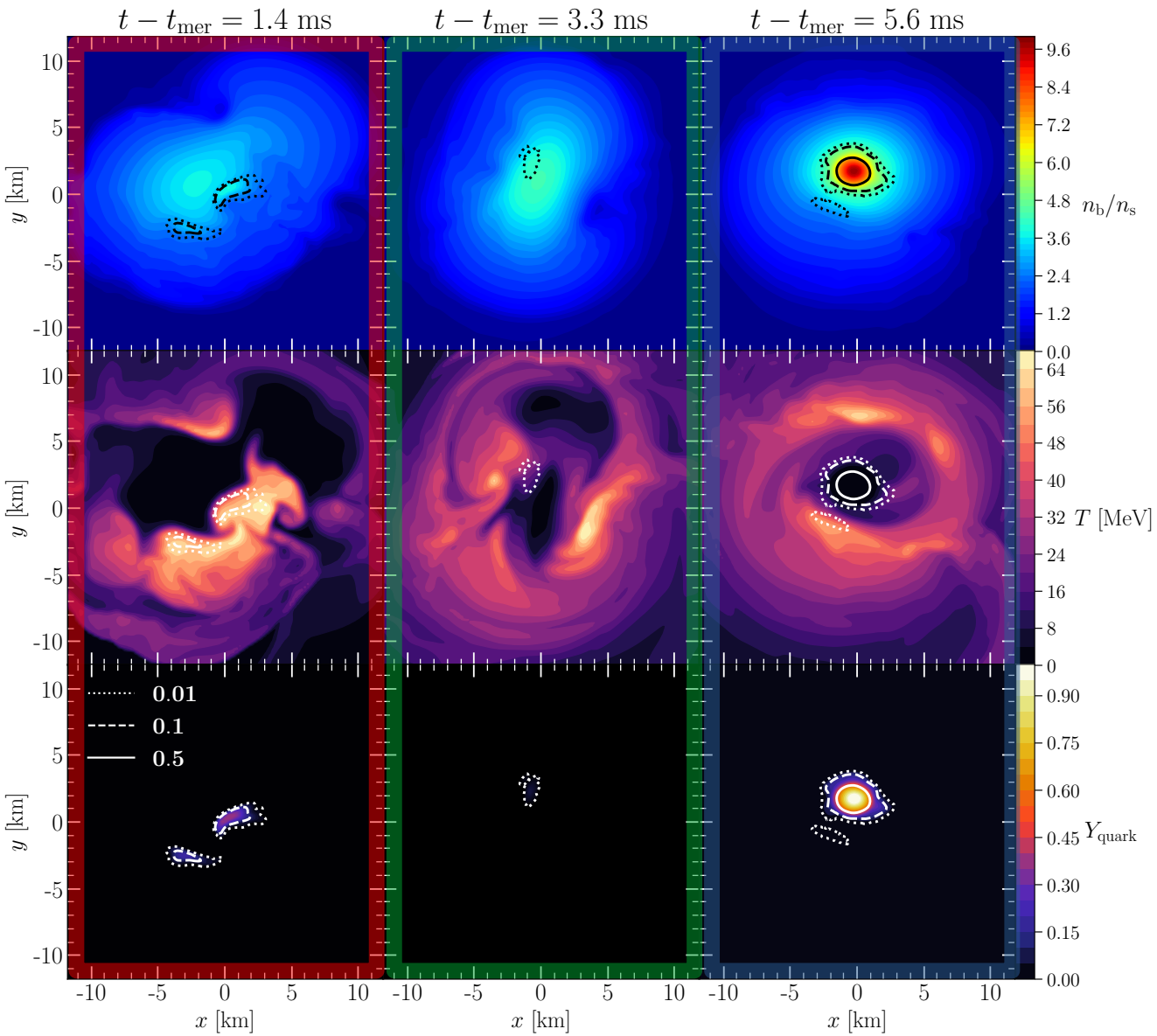

Tootle, CE, Topolski, Demircik, Järvinen, Rezzolla 2205.05691 (SciPost)

Phase Diagram

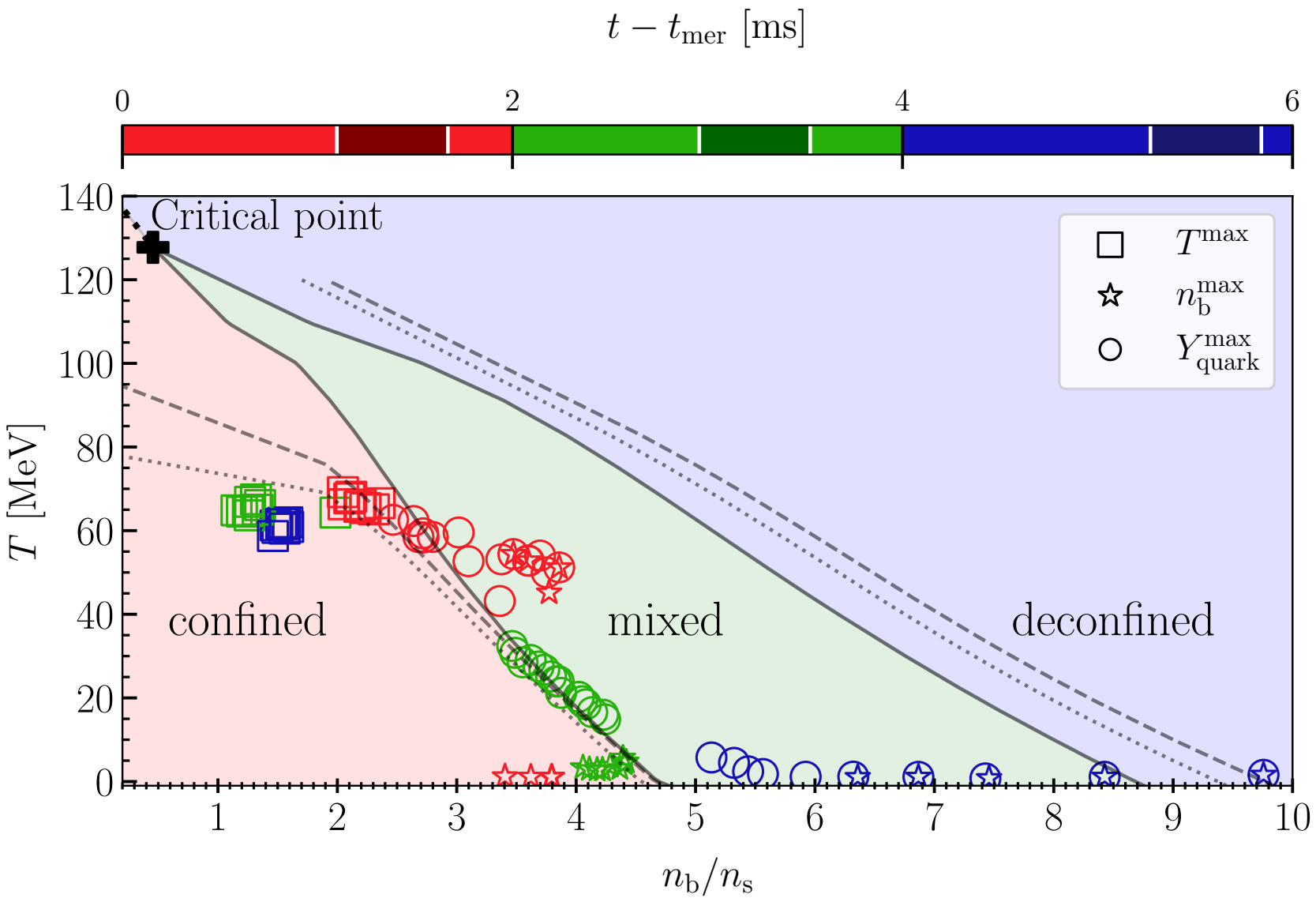

Tootle, CE, Topolski, Demircik, Järvinen, Rezzolla 2205.05691 (SciPost)

Quark Abundance

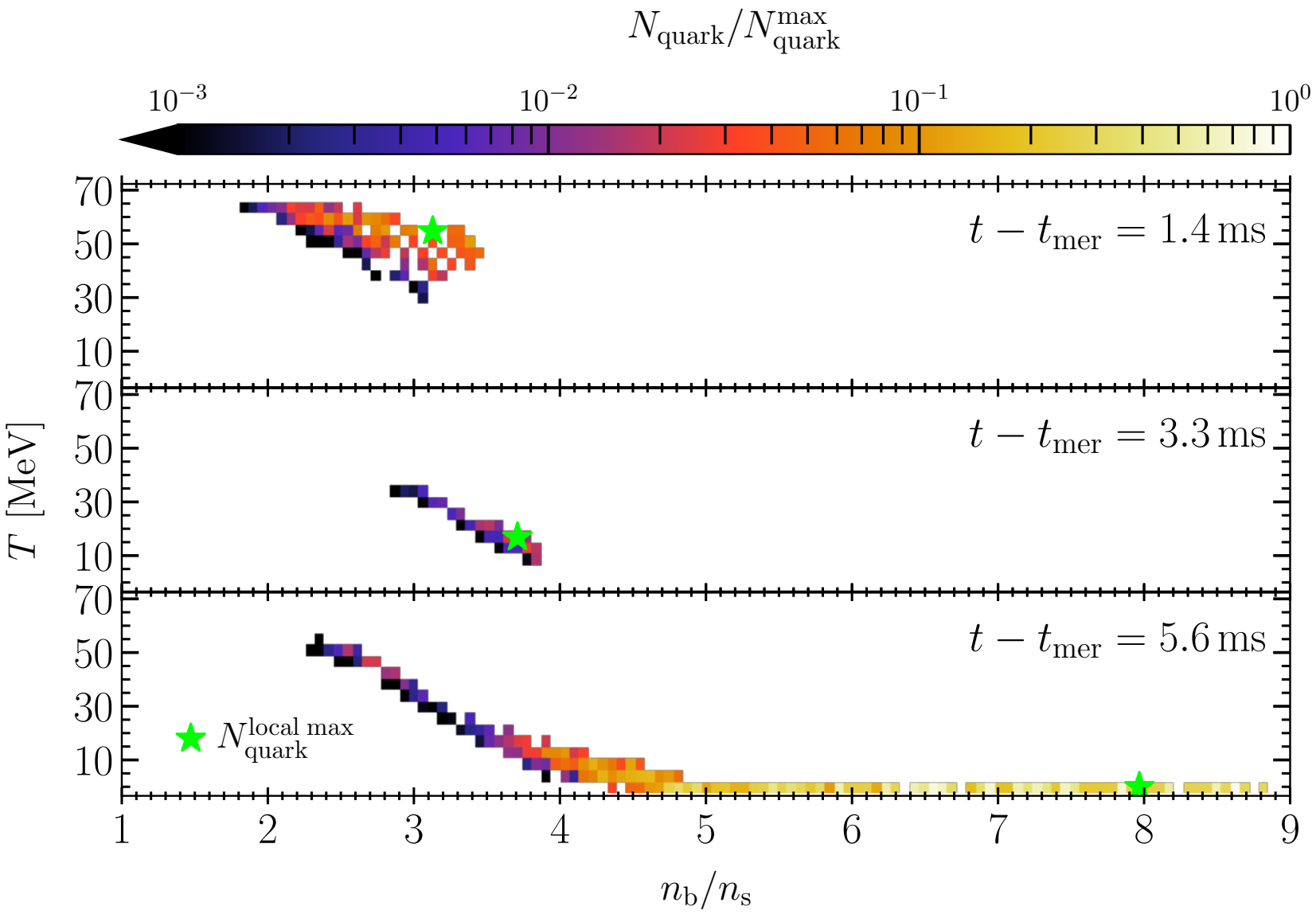

Tootle, CE, Topolski, Demircik, Järvinen, Rezzolla 2205.05691 (SciPost)

Extracting Waveforms

- Newman-Penrose scalar ψ_4 from simulation

$$\psi_4 := C_{\mu\nu\rho\sigma} k^\mu \bar{m}^\nu k^\rho \bar{m}^\sigma \,, \quad \text{null tetrade: } \{l^\mu, k^\mu, m^\mu, \bar{m}^\mu\} \,.$$

- GW polarization amplitudes (h_+,$h_\times$) are related to ψ_4 via

see e.g. book by M. Alcubierre (2005)

$$\ddot{h}_+ - i\ddot{h}_\times = \psi_4 = \sum_{\ell=2}^{\infty} \sum_{m=-\ell}^{\ell} \psi_4^{\ell m} {}_{-2}Y_{\ell m}(\theta, \varphi) \,.$$

- Consider for example the dominant $\ell = m = 2$ mode

$$h_{+,\times} = \sum_{\ell=2}^{\infty} \sum_{m=-\ell}^{\ell} h_{+,\times}^{\ell m} {}_{-2}Y_{\ell m}(\theta, \varphi) \approx h_{+,\times}^{22} {}_{-2}Y_{22}(\theta, \varphi) \,,$$

- Optimal orientation (${}_{-2}Y_{22}(0,0) = \frac{1}{2}\sqrt{5/\pi}$) with respect to the detector.
- Extrapolate signal to same luminosity distance ($40\,\mathrm{Mpc}$) as GW170817.

Power Spectral Density

Post-merger power spectral density (PSD) has typical three peak structure

$$\tilde{h}(f) \equiv \sqrt{\frac{|\tilde{h}_+(f)|^2 + |\tilde{h}_\times(f)|^2}{2}}\,, \quad \tilde{h}_{+,\times}(f) \equiv \int h_{+,\times}(t) e^{-i2\pi f t} dt\,.$$

Characteristic frequencies f_1, f_2, f_3 encode information about EOS.

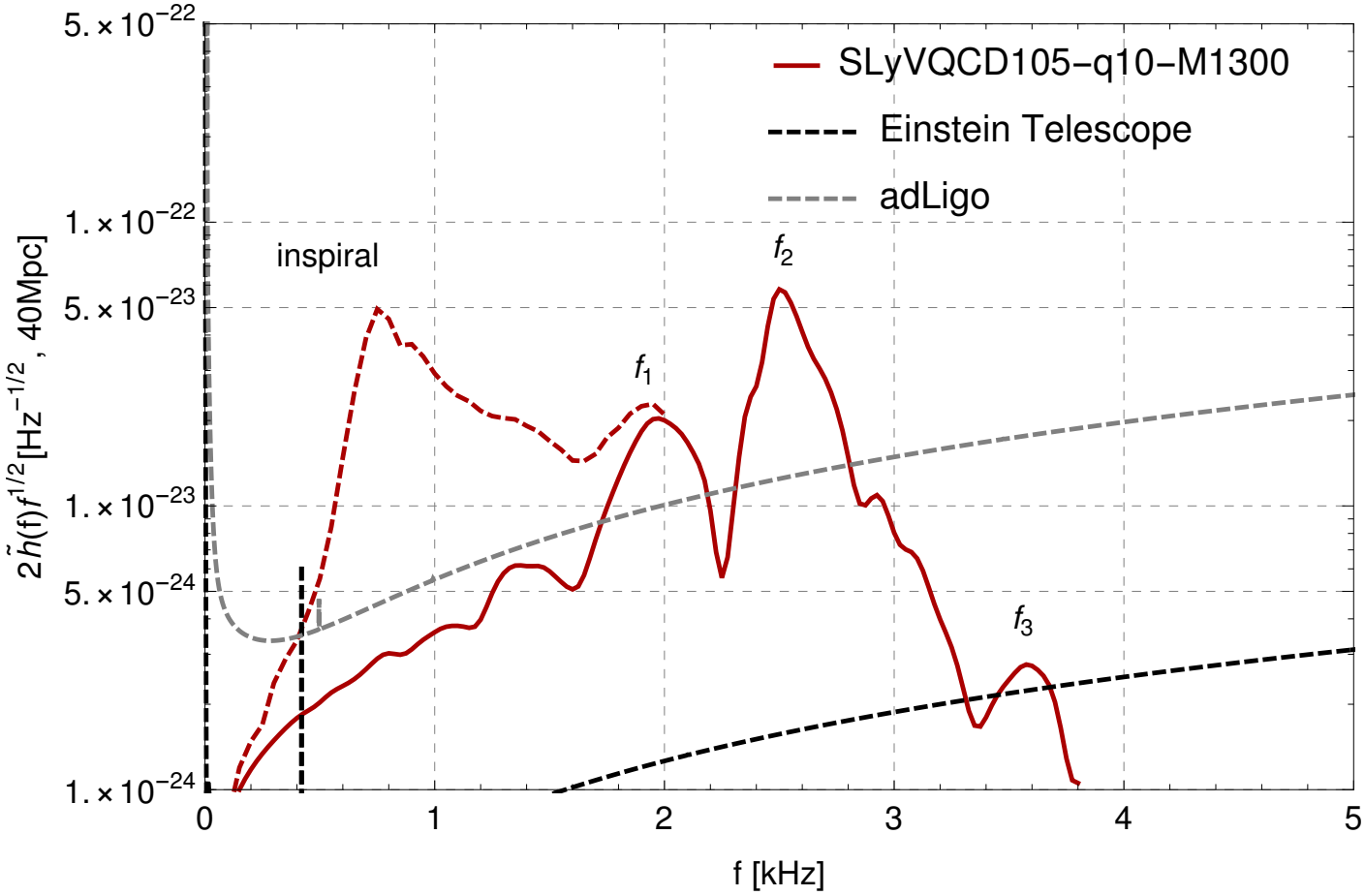

Waveforms and Frequency Spectra

- Small impact of quark matter on post-merger frequencies.

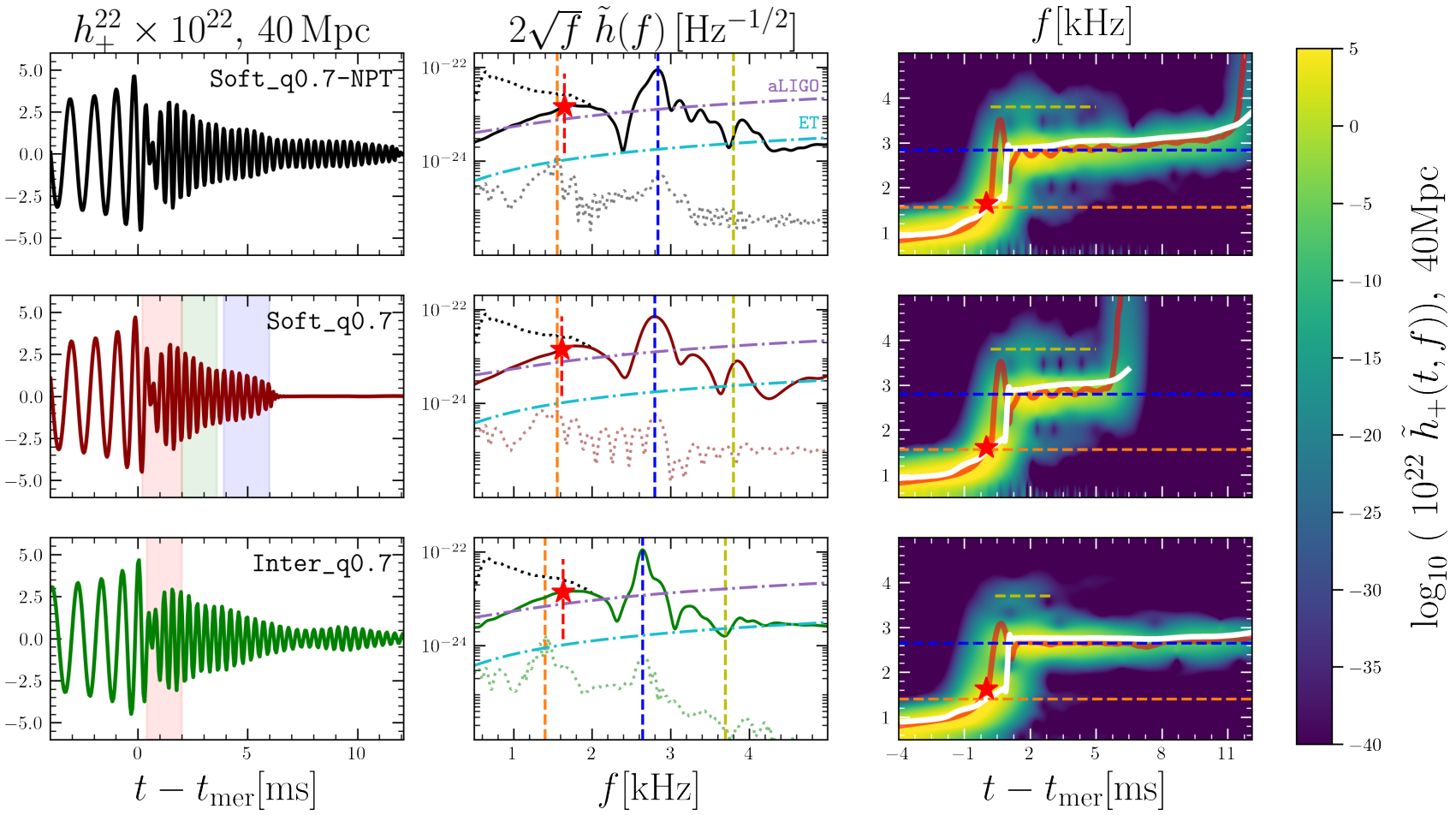

Tootle, CE, Topolski, Demircik, Järvinen, Rezzolla 2205.05691 (SciPost)

Waveforms and Frequency Spectra

- Small impact of quark matter on post-merger frequencies.
- Phase transition triggered collapse (PTTC) leads to shorter lifetime of the hyper massive neutron star (HMNS).

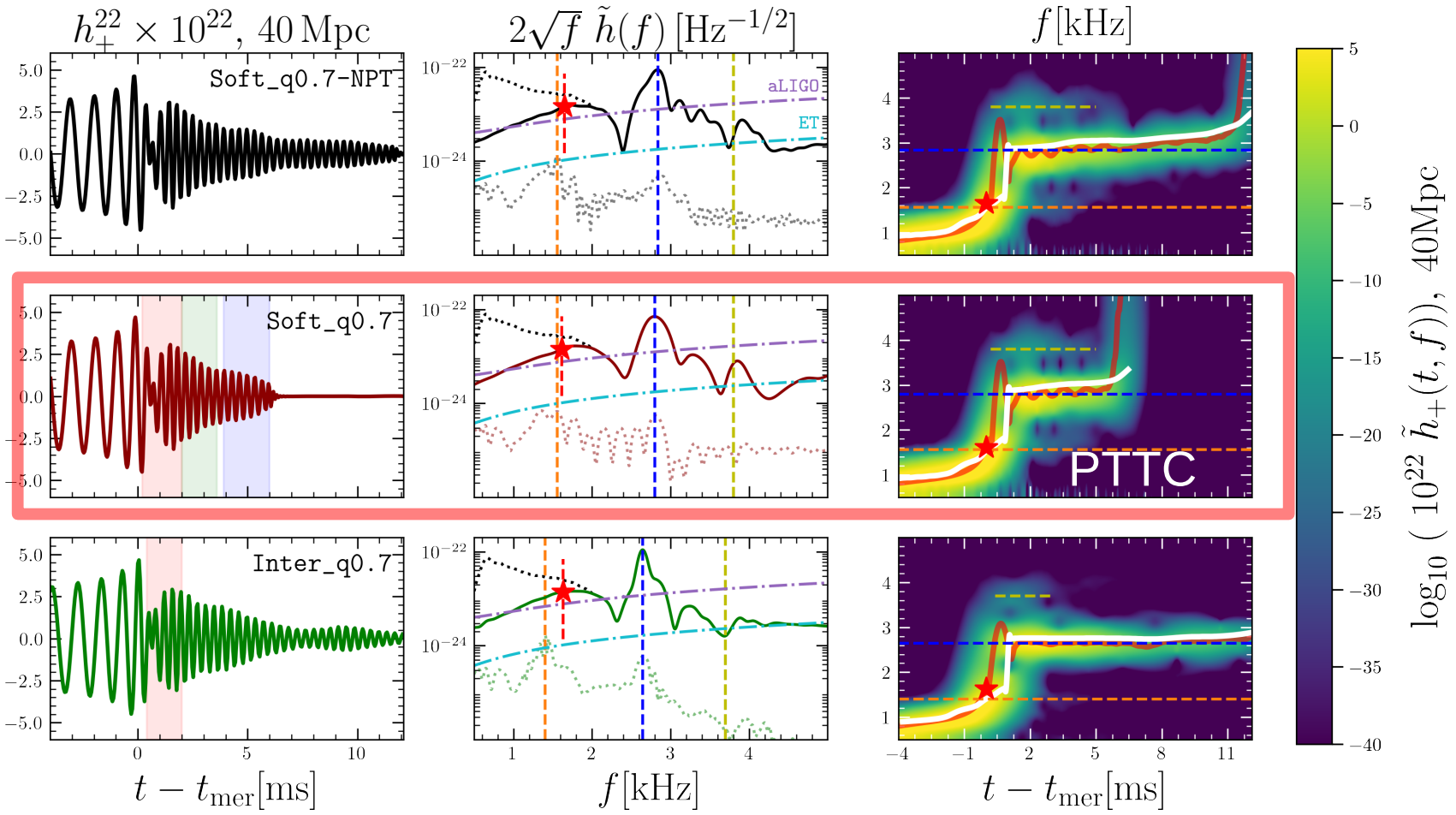

Tootle, CE, Topolski, Demircik, Järvinen, Rezzolla 2205.05691 (SciPost)

Summary

This talk:

- Basic properties of the cold EOS and neutron stars can be estimated from constraint sampling: $p(e)\,, M(R)\,, c_s^2\,, \tilde{\Lambda}(\mathcal{M}_{\rm chirp})\,, \ldots$
- Hot V-QCD hybrid EOS with deconfinement phase transition, three tabulated versions on CompOSE database: DEJ(DD2-VQCD).
- Predictions for the QCD critical point: https://compose.obspm.fr/

$$110\ \mathrm{MeV} \lesssim T_c \lesssim 130\ \mathrm{MeV}\,, \quad 0.3\ n_s \lesssim n_c \lesssim 0.6\ n_s\,.$$

- Neutron star merger simulations with V-QCD EOS.
- Identified 3 different stages in HMNSs: hot, warm, cold quark matter.
- Small impact on frequencies, but PTTC shortens HMNS lifetime.

Ongoing work:

- Further improving and constraining the V-QCD hybrid EOS models.
- Prompt collapse: Imprint of quark formation on threshold mass?
- Long-time stability (lifetime) of HMNS: Need simulations up to 1-2 sec. (expensive, simplified spacetime evolution, axial-symmetry, ...)
- ...

V-QCD without baryons (I)

Consider first the non-baryonic V-QCD action, whose solutions will serve as background for the probe baryons

$$S^{(0)}_{\mathrm{V-QCD}} = S_{\mathrm{glue}} + S^{(0)}_{\mathrm{DBI}}\,.$$

The gluon part is given by the IHQCD (dilaton gravity) action

$$S_{\mathrm{glue}} = N_c^2 M^3 \int d^5x \sqrt{-g}\left[R - \tfrac{4}{3}\tfrac{(\partial\lambda)^2}{\lambda^2} + V_g(\lambda)\right],$$

where $\lambda \equiv e^{\phi} \leftrightarrow \mathrm{Tr}F^2$ ($\approx g^2 N_c$ near the boundary) sources the 't Hooft coupling in YM theory, the dilaton potential is chosen[1] to mimic QCD

$$V_g(\lambda) = 12\left[1 + V_1\lambda + \tfrac{V_2\lambda^2}{1+\lambda/\lambda_0} + V_{\mathrm{IR}} e^{-\lambda_0/\lambda}(\lambda/\lambda_0)^{4/3}\sqrt{\log(1+\lambda/\lambda_0)}\right].$$

Finite T is implemented by homogeneous+isotropic black brane metric

$$ds^2 = e^{2A(r)}(-f(r)dt^2 + d\vec{x}^2 + f^{-1}(r)dr^2)\,.$$

[1] E.g. V_1 and V_2 are fixed by requiring the UV RG flow of the 't Hooft coupling to be the same as in QCD up to two-loop order.

V-QCD without baryons (II)

The flavor part is modelled by the tachyonic DBI-action[2]

$$S_{\rm DBI}^{(0)} = -N_f N_c M^3 \int d^5x V_{f0}(\lambda) e^{-\tau^2} \sqrt{-\det\left[g_{ab} + \kappa(\lambda)\partial_a\tau\partial_b\tau + w(\lambda)F_{ab}\right]}\,,$$

$$F_{rt} = \Phi'(r)\,, \quad \Phi(0) = \mu\,,$$

where the tachyon $\tau \leftrightarrow \bar{q}q$ controls chiral symmetry breaking.

Several potentials: $\{V_g(\lambda), V_{f0}(\lambda), w(\lambda), \kappa(\lambda)\}$, chosen to match pQCD in UV ($\lambda \to 0$), qualitative agreement with QCD in IR ($\lambda \to \infty$) and tuned to lattice QCD in the middle ($\lambda \sim \mathcal{O}(1)$).

For details see Appendix B of Ishii, Järvinen, Nijs arXiv:1903.06169

Different solutions:

without/with horizon $\leftrightarrow$ confined/deconfined phase
without/with tachyon $\leftrightarrow$ chirally symmetric/chirally broken phase

[2] Without baryons we have a vectorial flavor singlet gauge field $A^{(L/R)} = \mathbb{I}_f \Phi(r) dt$ giving nonzero charge density and chemical potential.

Probe baryons in V-QCD

Each baryon maps to a solitonic "instanton" configuration of non-Abelian gauge fields in the bulk.

Witten; Gross, Ooguri; ...

Consider the full non-Abelian brane action $S = S_{\rm DBI} + S_{\rm CS}$ where

Bigazzi, Casero, Cotrone, Kiritsis, Paredes; Casero, Kiritsis, Paredes

$$S_{\rm DBI} = -\frac{1}{2} M^3 N_c \, \mathbb{T}r \int d^5x \, V_{f0}(\lambda) e^{-\tau^2} \left(\sqrt{-\det \mathbf{A}^{(L)}} + \sqrt{-\det \mathbf{A}^{(R)}} \right) ,$$

$$\mathbf{A}^{(L/R)}_{MN} = g_{MN} + \delta^r_M \delta^r_N \kappa(\lambda) \tau'(r)^2 + \delta^{rt}_{MN} w(\lambda) \Phi'(r) + w(\lambda) F^{(L/R)}_{MN}$$

gives the dynamics of the solitons.
The Cern-Simons term sources the baryon number for the solitions

$$S_{\rm CS} = \frac{N_c}{8\pi^2} \int \Phi(r) e^{-b\tau^2} dt \wedge \left(F^{(L)} \wedge F^{(L)} - F^{(R)} \wedge F^{(R)} + \cdots \right) .$$

Non-Abelian DBI action only known to first few orders in $F^{(L/R)}$: expand to second order on top of solution $(g_{MN}, \Phi, \lambda, \tau)$ obtained from $S^{(0)}_{V-QCD}$.

Homogeneous Baryon Ansatz

Set $N_f = 2$ and consider the SU(2) Ansatz

Rozali, Shieh, Van Raamsdonk, Wu

$$A_L^i = -A_R^i = h(r)\sigma^i$$

Immediate consequence: baryon charge integrates to zero?

$$N_b \propto \int dr \frac{d}{dr}\left[e^{-b\tau^2} h^3 (1 - 2b\tau^2)\right] \stackrel{?}{=} 0$$

However finite baryon number may can be realized by discontinuity of h $\leftrightarrow$ smeared solitons in singular gauge.

Ishii, Järvinen, Nijs, arXiv:1903.06169

The free parameter b of the model is used to tune the baryon onset to its physical value in QCD.

Binary tidal deformability and chirp mass

- Chirp mass can be extracted accurately from inspiral GW strain signal

$$\mathcal{M}_{chirp} = \frac{(M_1 M_2)^{3/5}}{(M_1 + M_2)^{1/5}} = \left(\frac{5}{96}\pi^{-8/3} f^{-11/3} \dot{f}\right)^{3/5} . \tag{2}$$

- Binary tidal deformability encodes EOS properties via Λ_i

$$\tilde{\Lambda} = \frac{16}{13} \frac{(12M_2 + M_1)\, M_1^4 \Lambda_1 + (12M_1 + M_2)\, M_2^4 \Lambda_2}{(M_1 + M_2)^5} . \tag{3}$$

- GW170817 only "good" event so far:

$$\mathcal{M}_{chirp} = 1.188^{+0.004}_{-0.002} M_\odot, \quad q = M_2/M_1 > 0.7, \quad \tilde{\Lambda} \lesssim 720 . \tag{4}$$

LIGO/Virgo: arXiv:1805.11579

Mechanical Toy Model

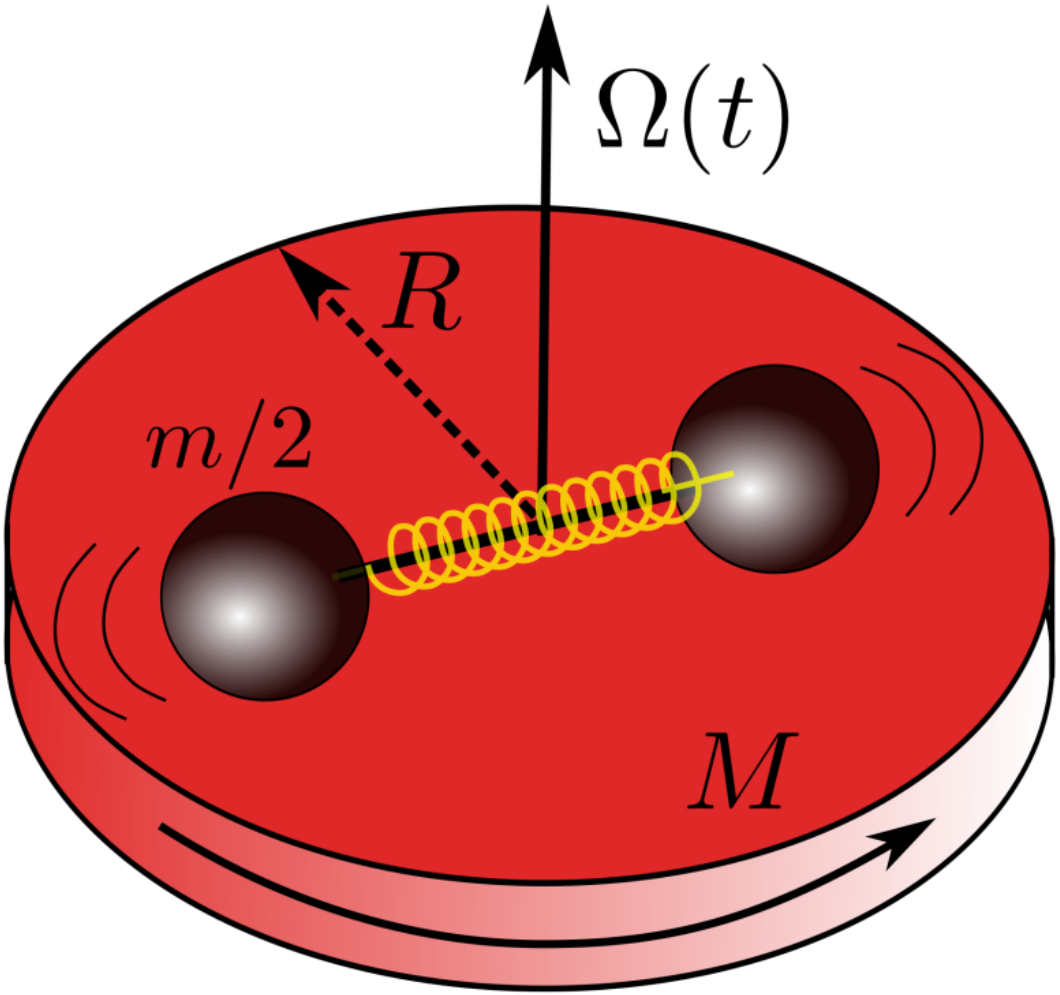

Takami, Rezzolla, Baiotti arXiv:1412.3240

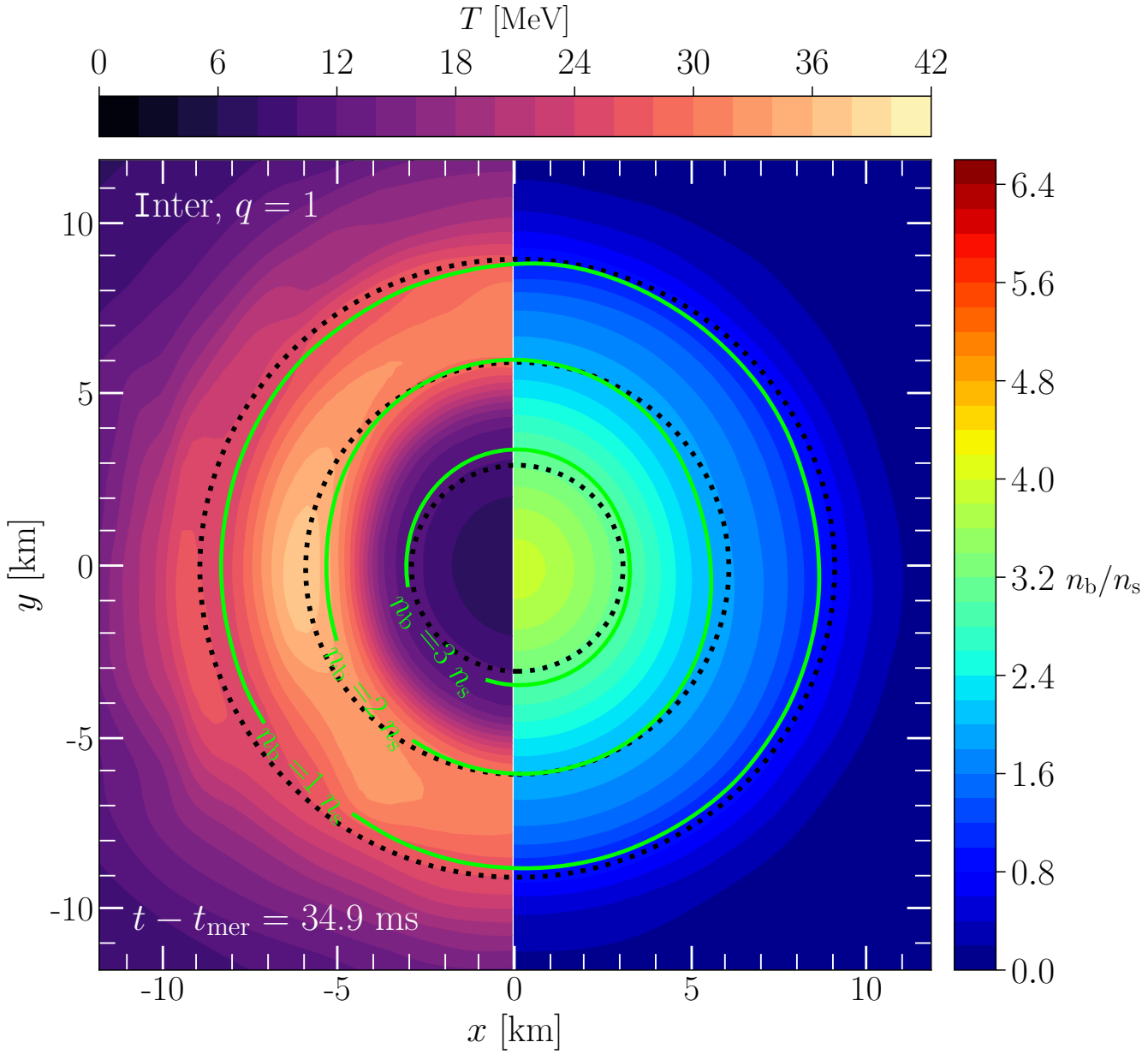
T [MeV]
0
6
12
18
24
30
36
42
Inter, q = 1
t − t_mer = 34.9 ms
n_b = 3 n_s
n_b = 2 n_s
n_b = 1 n_s
y [km]
x [km]
10
5
0
-5
-10
6.4
5.6
4.8
4.0
3.2 n_b/n_s
2.4
1.6
0.8
0.0

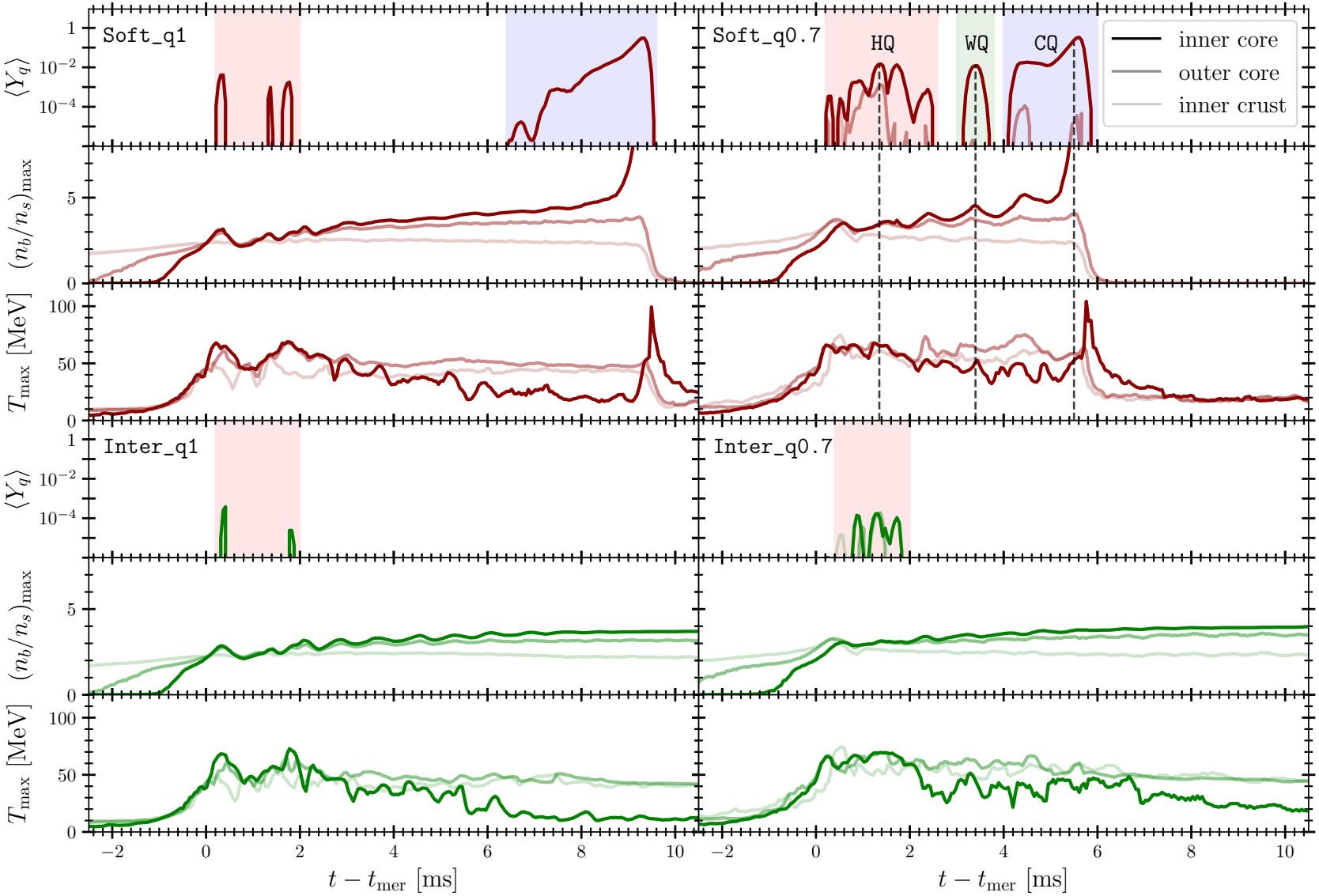
Soft_q1
Soft_q0.7
HQ
WQ
CQ
inner core
outer core
inner crust
Inter_q1
Inter_q0.7
$\langle Y_q \rangle$
$(n_b/n_s)_{\max}$
$T_{\max}$ [MeV]
$t - t_{\mathrm{mer}}$ [ms]

Phase Transition Signatures in Wavefrom Spectra

- **NPT:** No Phase Transition
- **PTTC:** Phase Transition Triggered Collapse
- **DPT:** Delayed Phase Transition

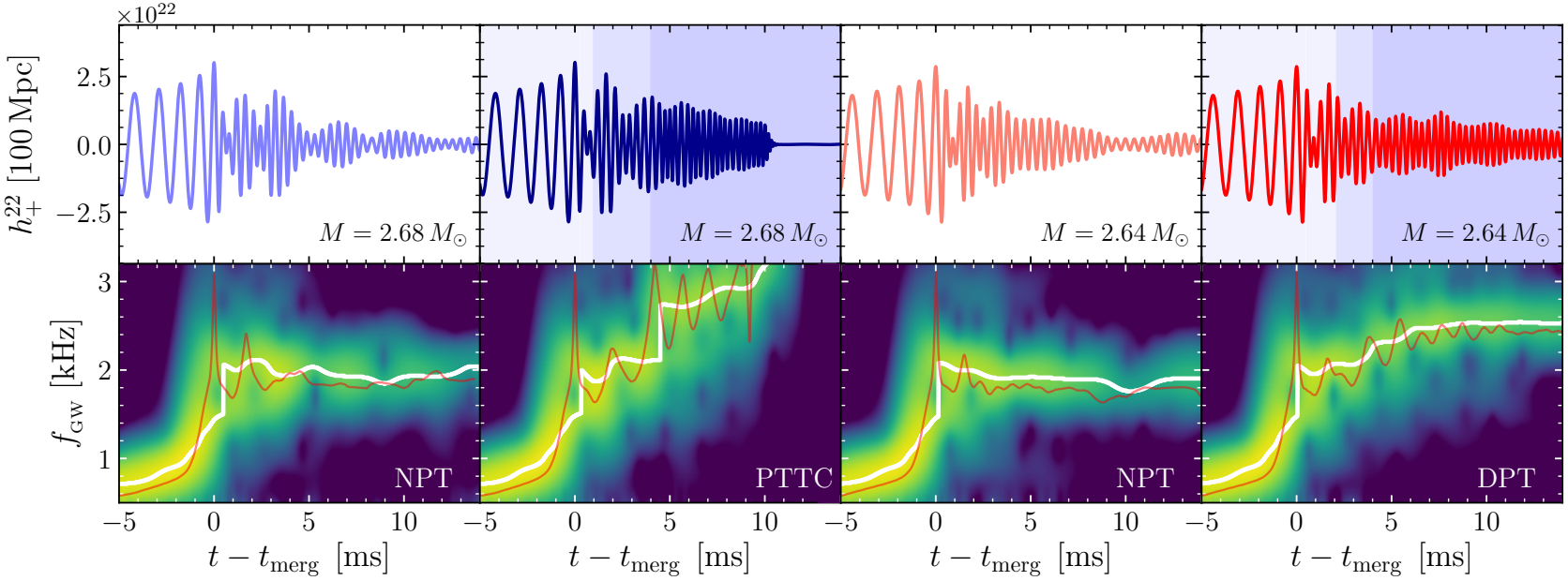

Weih, Hanauske, Rezzolla arXiv:1912.09340

Finite Temperature Extension

- Temperature dependence is essential when studying BNS-mergers.
- T-dependence of V-QCD baryons is trivial: confining background has no horizon, artefact of large N_c limit.
- Van der Waals construction to extend cold V-QCD baryons to finite-T.
- Ideal gas of protons, neutrons and electrons with excluded volume correction for nucleons.

  $$p_{\rm ex}(T,\{\mu_i\}) = p_{\rm id}(T,\{\tilde{\mu}_i\})\,, \quad \tilde{\mu}_i = \mu_i - v_0 p_{\rm ex}(T,\{\mu_i\}) \quad (i = p,\, n)$$
- Add potential term to match with V-QCD at $T = 0$

$$p_{\rm vdW}(T,\{\mu_i\}) = p_{\rm ex}(T,\{\mu_i\}) + \Delta p(\{\mu_i\})$$

$$\Delta p(\{\mu_i\}) = p_{\rm V-QCD}(T=0,\{\mu_i\}) - p_{\rm ex}(T=0,\{\mu_i\})$$

Rischke, Gorenstein, Stoecker, Greiner, Z Phys. C 51, 485 (1991)

Vovchenko, Gorenstein, Stoecker, arXiv:1609.03975

Vovchenko, Motornenko, Alba, Gorenstein, Satarov, Stoecker, arXiv:1707.09215

Building blocks of the EOSs

- Lowest densities ($0 - 0.5\, n_s$): Baym-Pethick-Sutherland (BPS) EOS

  Baym, Pethick, Sutherland (1971)

- Low densities ($0.5 - 1.2\, n_s$): $p(n) = K\, n^{\Gamma}\,, \quad \Gamma \in [1.77, 3.23]$

  Hebeler, Lattimer, Pethick, Schwenk arXiv:1303.4662

- High densities ($1.2 - 40\, n_s$): speed of sound parametrization

  Annala, Gorda, Kurkela, Nättilä, Vuorinen arXiv:1903.09121

- Highest densities ($\gtrsim 40\, n_s$): perturbative QCD results

$$p(\mu) = \frac{3}{4\pi^2}\left(\frac{\mu}{3}\right)^4 \left(c_1 - \frac{d_1 X^{-\nu_1}}{\mu/GeV - d_2 X^{-\nu_2}}\right)\,, \quad X \in [1,4]\,, \qquad (5)$$

$$c_1 = 0.9008 \quad d_1 = 0.5034 \quad d_2 = 1.452 \quad \nu_1 = 0.3553 \quad \nu_2 = 0.9101\,.$$

Kurkela, Romatschke, Vuorinen arXiv:0912.1856; Fraga, Kurkela, Vuorinen arXiv:1311.5154

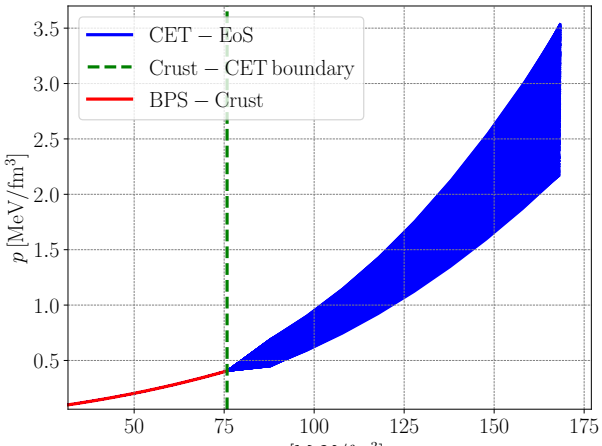

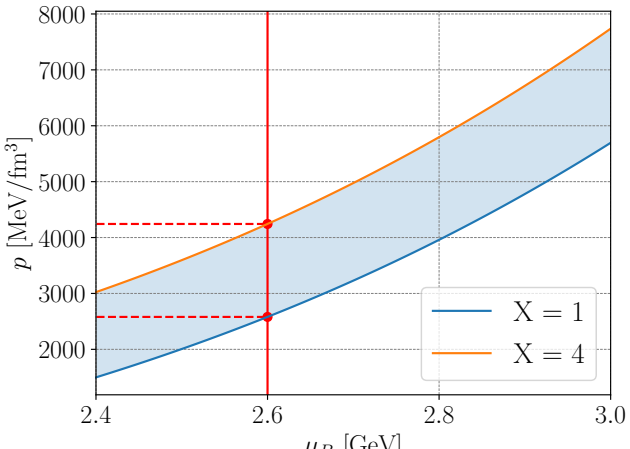

Two Puzzles

- *Is there a micro-physical model that can explain the agnostic sound-speed profile inside neutron stars?*
- *What is the reason for the strong tension between the HESS J1731-347 measurement and model agnostic M-R distribution?*

$$M = 0.77^{+0.20}_{-0.17}\, M_\odot\,, \quad R = 10.4^{+0.86}_{-0.78}\,\mathrm{km}\,.$$

Doroshenko, Suleimanov, Pühlhofer, Santangelo (Nature Astronomy Oct.2022)

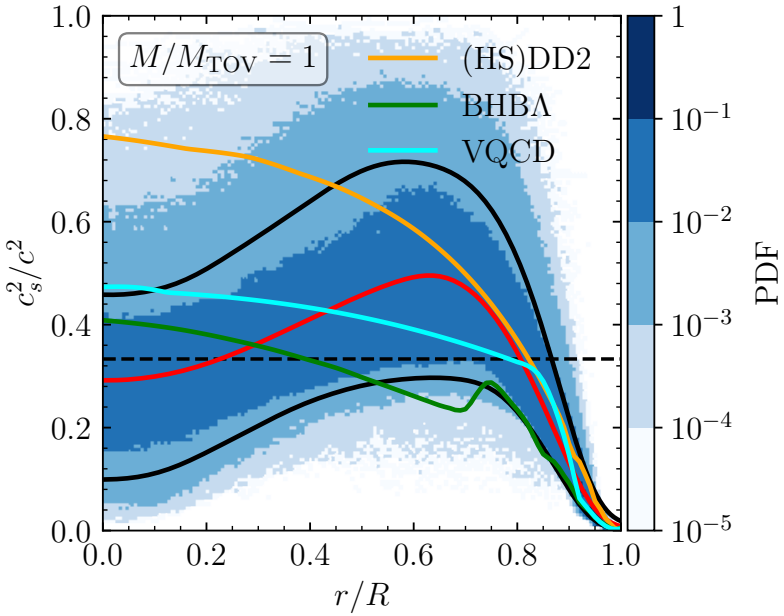

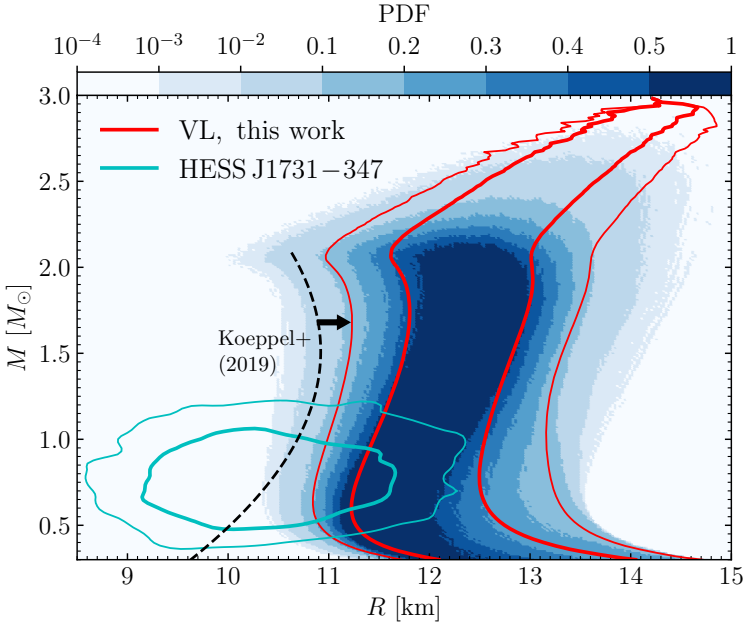

CE, Rezzolla 2207.04417 (ApJL), Jiang, CE, Rezzolla 2211.00018

Two Puzzles

- *Is there a micro-physical model that can explain the agnostic sound-speed profile inside neutron stars?*
- *What is the reason for the strong tension between the HESS J1731-347 measurement and model agnostic M-R distribution?*
- Combined estimate with agnostic Bayesian analysis:

$$M = 0.77\, M_\odot\,, \quad R = 11.43^{+0.64}_{-0.60}\,\mathrm{km}\,.$$

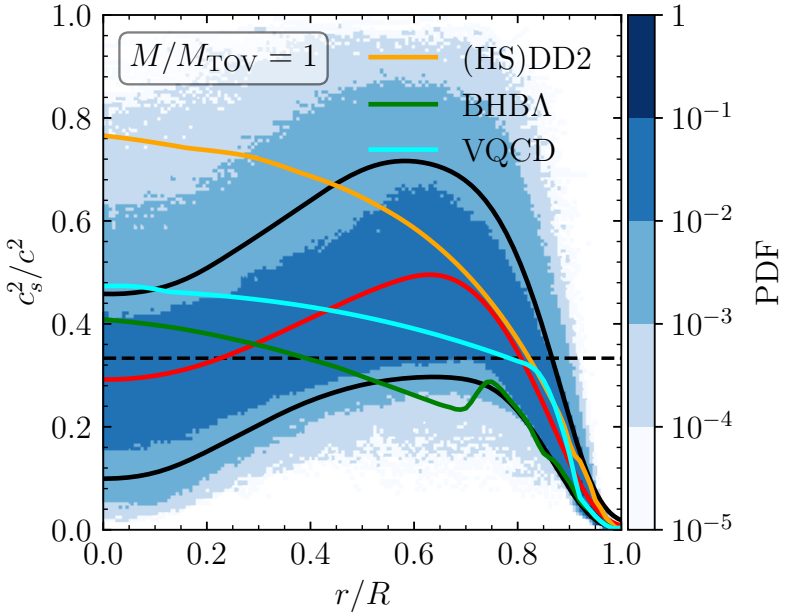

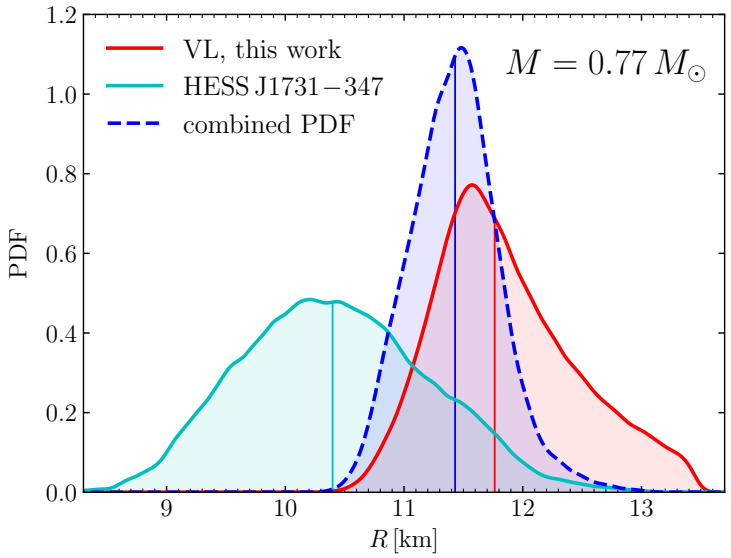

CE, Rezzolla 2207.04417 (ApJL), Jiang, CE, Rezzolla 2211.00018